

Fundamental Limits of Wireless Caching Under Mixed Cacheable and Uncacheable Traffic

Hamdi Joudeh, Eleftherios Lampiris, Petros Elia and Giuseppe Caire

Abstract

We consider cache-aided wireless communication scenarios where each user requests both a file from an a-priori generated cacheable library (referred to as ‘content’), and an uncacheable ‘non-content’ message generated at the start of the wireless transmission session. This scenario is easily found in real-world wireless networks, where the two types of traffic coexist and share limited radio resources. We focus on single-transmitter, single-antenna wireless networks with cache-aided receivers, where the wireless channel is modelled by a degraded Gaussian broadcast channel (GBC). For this setting, we study the delay-rate trade-off, which characterizes the content delivery time and non-content communication rates that can be achieved simultaneously. We propose a scheme based on the separation principle, which isolates the coded caching and multicasting problem from the physical layer transmission problem. We show that this separation-based scheme is sufficient for achieving an information-theoretically order optimal performance, up to a multiplicative factor of 2.01 for the content delivery time, when working in the generalized degrees of freedom (GDoF) limit. We further show that the achievable performance is near-optimal after relaxing the GDoF limit, up to an additional additive factor of 2 bits per dimension for the non-content rates. A key insight emerging from our scheme is that in some scenarios considerable amounts of non-content traffic can be communicated while maintaining the minimum content delivery time, achieved in the absence of non-content messages; compliments of ‘topological holes’ arising from asymmetries in wireless channel gains.

H. Joudeh, E. Lampiris and G. Caire are with the Communications and Information Theory Group, Faculty of Electrical Engineering and Computer Science, Technische Universität Berlin, 10587 Berlin, Germany (e-mail: h.joudeh@tu-berlin.de; caire@tu-berlin.de; lampiris@tu-berlin.de). P. Elia is with the Communication Systems Department, EURECOM, 06410 Sophia Antipolis, France (e-mail: elia@eurecom.fr).

This work is supported in part by the European Research Council (ERC) under the ERC grant agreement N. 789190 (project CARENET), and the ERC grant agreement N. 725929 (project DUALITY).

1 Introduction

Cache-aided architectures have emerged as an essential next step in the evolution of communication networks [1]. This is backed by two key factors: the explosion in *cacheable* data traffic due to on-demand access to internet content (e.g. video-streaming); and the low cost and ubiquity of large on-board storage memory. In the caching paradigm, popular content is pro-actively stored across network nodes during off-peak times, when network resources are underutilized; and then the pre-stored content is leveraged to alleviate the traffic load during congested peak times [2].

The recent few years saw the emergence of information-theoretic studies that aim at establishing the fundamental limits of communication over cache-aided networks, initiated by Maddah-Ali and Niesen in [3]. For an idealized symmetric broadcast channel (BC), in which cache-equipped users (receivers) are connected to a server (transmitter) through a noiseless shared link, Maddah-Ali and Niesen showed that a novel *coded* caching and multicasting scheme can serve an arbitrarily large number of users with finite resources (e.g. time and bandwidth). The achievable performance in [3], characterized in terms of the shared link *normalized load*,¹ was shown to be order optimal in the information-theoretic sense, i.e. within a constant multiplicative factor of the ultimate performance. The information-theoretic optimality result in [3] was tightened later on in [4, 5] under the restriction of uncoded cache placement, and in [6] for the general unrestricted case.

1.1 Wireless caching

The bulk of data traffic nowadays is generated for wireless and mobile devices, a trend foreseen to continue and grow in forthcoming years. This has driven a surge of interest in extending the information-theoretic coded caching paradigm to wireless network settings. Such settings differ from their idealized counterparts (e.g. [3, 7]) in several important aspects, which most notably include: the noisiness of wireless channels; the uneven and asymmetric nature of wireless network topologies; and the crucial impact of fading and channel state information (CSI) feedback.

In the context of single-transmitter networks, the coded caching paradigm has been extended to noisy settings, including erasure and degraded BCs [8–16], and multi-antenna BCs [17–25]. For multi-transmitter settings, coded caching has been studied in device-to-device (D2D) networks [26], interference networks with caches at the transmitters only or at both transmitters and receivers [27–33], and fog radio access networks (F-RANs) [34, 35], among other settings. While many of the above works focus on symmetric topologies for simplicity, aspects specific to uneven topologies were studied in [10–16, 20, 23]. The interplay between CSI feedback and coded caching in multi-antenna and multi-transmitter networks has been investigated in [17–22, 32, 33]. Moreover, some recent works explore the role of multi-antenna transmitters and shared receiver caches in alleviating the subpacketization complexity bottleneck of coded caching and multicasting schemes [36, 37].

1.2 Mixed cacheable and uncacheable traffic

All the above-mentioned works consider scenarios in which the network carries a single type of traffic that takes the form of (popular) content drawn from an a-priori generated library (or database). This approach has been very useful and successful in gaining insights into the fundamental limits of cache-aided wireless networks, and the design of optimal and near optimal coded caching and multicasting schemes. Nevertheless, wireless data traffic does not comprise of only *cacheable* content. *Uncacheable* non-content traffic, generated from interactive applications, as well as voice and

¹This can also be seen as a *normalized delivery time* (NDT) measure, where one unit of time (i.e. time slot) is equivalent to the time required to deliver a single file in the absence of caches.

video calls, to name a few examples, also constitutes a significant portion of overall wireless data traffic (estimated as 40 percent [38]). Moreover, content popularity profiles in reality are far from static and may change on a daily or even hourly basis [1, 38]. Therefore, newly generated content can be both in very high demand as well as not yet registered or available in caches.

Motivated by the mixed nature of data traffic, we initiate the study of cache-aided wireless networks with both *cacheable* and *uncacheable* types of traffic. Throughout this work, we use *content* traffic to describe pre-generated *cacheable* files; and *non-content* traffic to describe *uncacheable* messages, instantaneously generated at the start of wireless transmission sessions. These definitions are further clarified below and in Section 2, where the problem setting is formally described.

1.3 Considered setting and adopted approach

The setting of focus is a cache aided degraded Gaussian BC (GBC), comprising a single transmitter and K receivers. The transmitter has access to a pre-generated content library of N equal-size files, while each user has a cache memory that can store content of size equal to the size of M files during a *placement phase*, which takes place before communication sessions commence. The normalized cache size is defined as $\mu \triangleq \frac{M}{N}$, where $\mu \in [0, 1]$. At the beginning of a communication session, known as a *delivery phase*, each user requests a content file, as well as an instantaneously generated non-content message, not known a-priori to the transmitter. The setup is illustrated in Fig. 1.

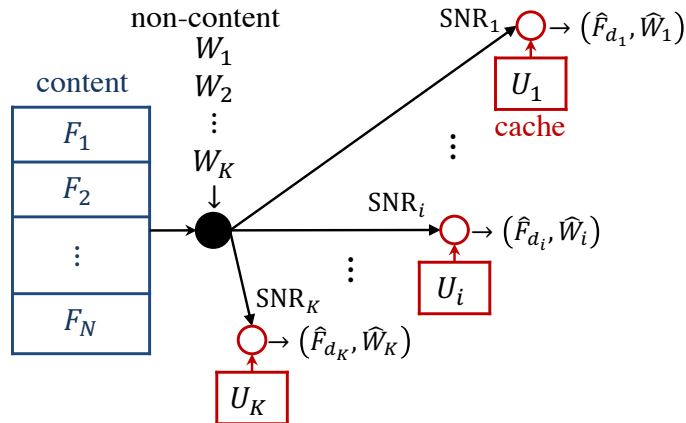


Figure 1: K -user cache-aided degraded GBC with a content library and non-content messages.

To gain initial insights, let us consider a symmetric physical channel special case with equal signal-to-noise ratio (SNR) across users. We start by taking non-content messages out of the picture, and focus on the delivery of K distinct content files.² In this case, the original Maddah-Ali and Niesen coded caching and multicasting scheme (referred to as the MN scheme henceforth) [3], coupled with a standard channel coding argument, achieves a (per-bit) communication delay of

$$\mathcal{T} = \frac{1}{\log(1 + \text{SNR})} \cdot \frac{K(1 - \mu)}{1 + K\mu}. \quad (1)$$

The above measure of delay corresponds to the number of (physical) channel uses required to deliver one bit of content for each user, in the Shannon limit (i.e. as the file size approaches infinity).

Now consider the additional transmission of K non-content messages, each intended to a unique user, at possibly distinct communication rates of R_1, \dots, R_K . The physical channel is now shared

²Here we assume that $N \geq K$ for ease of exposition. This assumption is relaxed further on.

between multicast messages (coded content) and unicast messages (non-content), such that

$$R_{[K]} + \sum_{i=1}^K R_i \leq \log(1 + \text{SNR}) \quad (2)$$

where $R_{[K]}$ denotes the rate of communicating multicast messages over the wireless channel. For any tuple of non-content rates (R_1, \dots, R_K) , we can achieve a communication delay of³

$$\mathcal{T}(R_1, \dots, R_K) = \frac{1}{(\log(1 + \text{SNR}) - \sum_{i=1}^K R_i)^+} \cdot \frac{K(1 - \mu)}{1 + K\mu}. \quad (3)$$

The delay-rate trade-off in (3) is achieved by employing a *separation* approach, which separates the coded caching and multicasting problem from the physical channel transmission problem, see, e.g., [31]. In particular caching, generating coded multicast messages and recovering requested files from received coded messages and local cache contents are carried out at the bit level in the standard shared link fashion, using the MN scheme [3]. On the other hand, in this same separation approach, the physical-layer sees a collection of multicast messages and unicast messages, and communicates them using standard channel coding. As it turns out, the trade-off in (3) is order optimal, i.e. within a constant multiplicative factor from the information-theoretic trade-off (see Section 6).

The reader may have noticed that as far as the physical channel is concerned, the rates in (2) can be achieved using time-sharing, i.e. multicast and unicast messages are mapped into independent signals, communicated sequentially over distinct time slots. As one would imagine, the sufficiency of time-sharing in this setting is by virtue of symmetry. In general, time-sharing is rendered sub-optimal by the superposition and asymmetric nature of wireless channels, epitomized through the degraded GBC—one may envisage the superiority of superposition coding in asymmetric scenarios. Nevertheless, the current treatment in the literature of delivering content and non-content traffic as two independent problems, necessarily leads to time-sharing-like schemes, where the two types of traffic are scheduled on orthogonal physical-layer resource blocks. As we will see in this paper, this orthogonalization is suboptimal in general, specifically in asymmetric settings.

We propose to treat the two problems jointly. In particular, while we maintain a separation architecture that isolates coded caching and multicasting from physical-layer transmission, the transmission of messages corresponding to content and non-content traffics over the physical channel is carried out in a joint (non-orthogonal) manner, by leveraging power control with superposition coding and successive decoding. This leads to an order optimal performance in the information-theoretic sense, as we later show in this paper.

1.4 Generalized degrees of freedom regime

Attempting to settle the above question by pursuing *exact* delay-rate trade-off characterizations is bound to yield intricate solutions, which are not necessarily malleable or useful for analysis and gaining practical insights. To see this, let us consider a simple setting with $K = N = 2$ and $M = 1$. In this case, we know from the MN scheme that the delivery of one coded multicast message of normalized size given by $\frac{K(1-\mu)}{1+K\mu} = 1/2$ is sufficient to satisfy distinct user demands.

Using the above-described separation approach, we achieve a delay-rate trade-off of

$$\mathcal{T}(R_1, R_2) = \frac{1}{R_{12}} \cdot \frac{1}{2} \quad (4)$$

³We are interested in the total delay of the entire communication session, i.e. the time required to deliver both content files and non-content messages, in channel uses normalized by the number of file bits—see Section 2.2.

for any non-negative rate tuple (R_1, R_2, R_{12}) that satisfies

$$\begin{aligned} R_{12} + R_1 &\leq \log \left(1 + \frac{q \text{SNR}_1}{1 + \bar{q} \text{SNR}_1} \right) \\ R_2 &\leq \log (1 + \bar{q} \text{SNR}_2) \end{aligned} \quad (5)$$

for some power control variables $q \in [0, 1]$ and $\bar{q} \triangleq 1 - q$, under a unit average power constraint. Note that in the above, we assume without loss of generality that $\text{SNR}_1 \leq \text{SNR}_2$. The inequalities in (5) characterize the capacity region of the 2-user degraded GBC with unicast and multicast (i.e. common) messages. This region, and hence the delay achieved by separation in (4), crucially depend on the auxiliary power control variable q , and in general cannot be expressed explicitly in terms of fixed channel parameters only (i.e. SNR_1 and SNR_2). This dependency on auxiliary power control variable(s) becomes more problematic in larger networks with arbitrary K , where the physical channel communicates multiple nested sets of multicast messages, giving rise to delay-rate characterizations which are difficult to analyse. Effects of this complexity are seen through previous results on coded caching in the degraded GBC, see, e.g., [10–12].

In this work, we circumvent the above-described complexity issue by taking a step back from the *exact* delay-rate trade-off, and instead pursuing an *approximate* characterization based on the *generalized degree of freedom* (GDoF) measure [39]. In the GDoF sense, the capacity region of the physical channel in (5) reduces to all non-negative GDoF tuples (r_1, r_2, r_{12}) that satisfy

$$\begin{aligned} r_{12} + r_1 &\leq \alpha_1 \\ r_{12} + r_1 + r_2 &\leq \alpha_2 \end{aligned} \quad (6)$$

where α_1 and α_2 are GDoF-type channel strength parameters that correspond to SNR_1 and SNR_2 , respectively (see Section 2.1). The GDoF region in (6) is a polyhedron, and has the desirable property of admitting a reduced explicit description in terms of fixed channel parameters only (i.e. α_1 and α_2), without the need for auxiliary power control variables. From (6), the *generalized normalized delivery time* (GNDT), i.e. the GDoF counterpart of the delay in (4), is given by

$$\tau = \max \left\{ \frac{1}{(\alpha_1 - r_1)^+}, \frac{1}{(\alpha_2 - (r_1 + r_2))^+} \right\} \cdot \frac{1}{2} \quad (7)$$

obtained from the MN scheme and (6) by observing that for any non-content GDoF tuple (r_1, r_2) , a multicast GDoF of $r_{12} = \max \left\{ \frac{1}{(\alpha_1 - r_1)^+}, \frac{1}{(\alpha_2 - (r_1 + r_2))^+} \right\}$ is achievable. As we will see in Section 6, the simplicity of the linear inequalities in (6) allows for a direct comparison with counterpart information-theoretic outer bounds, from which we prove order optimality.

The explicit nature of the above GNDT-GDoF trade-off allows for deriving useful operational insights. For instance, (7) suggests that we can communicate a non-content message at a GDoF of $r_2 \leq \alpha_2 - \alpha_1$ to user 2, while simultaneously maintaining the GNDT achieved in the absence of non-content messages. As we will see in Section 3, the GNDT-GDoF trade-off allows us to precisely quantify the gains due to the asymmetry in channel strengths for an arbitrary number of users. Through these *topological holes* that appear as a result of asymmetry, we can communicate non-content messages at no cost in content delivery time. Moreover, we will also see that the GNDT-GDoF characterization leads to an approximate delay-rate characterization, up to a small gap. A detailed exposition of the main results and insights is given in Section 3.

1.5 Overview of contributions and related works

We conclude this section by highlighting the contributions of this work and relationship to prior art. In the main result of this paper (Theorem 1, Section 3), we obtain an achievable GNDT-GDoF

trade-off for the cache-aided degraded GBC with mixed content and non-content traffic; and we prove that this trade-off is order optimal in the information-theoretic sense, up to a multiplicative factor of 2.01. Furthermore, we show that the GNDT-GDoF characterization leads to a counterpart delay-rate trade-off, which is information-theoretically optimal up to a multiplicative factor of 2.01 for the content delay, and an additive factor of 2 bits (per dimension) for the non-content rates, at all finite SNR values (i.e. after relaxing the GDoF limit).

The achievability of our result is based on the separation principle, where the coded caching side of the problem is separated from the physical-layer communication side. This separation approach gives rise to a new physical-layer problem concerning the characterization of the GDoF and capacity regions of the K -user degraded GBC with unicast and multiple multicast message sets. We give a complete characterization of the GDoF region of this channel, and its capacity region up to a constant additive gap (see Section 4). This result may be of interest in its own right.

The converse proof of our main result is based on a non-trivial augmentation of the argument by Yu et al. [6], proposed for the idealized shared link setting. Guided by separation in the achievability scheme, we devise a sequence of steps that separate the information-theoretic bounds into a set of terms that capture the physical channel capacity, and a second set of terms that capture the load due to the content caching and delivery. The former are bounded by extending classical properties of the degraded BC, while the latter are bounded by invoking techniques from [6].

Related works: As a special case of our result, we recover the previous result in [16], where a similar setting was considered in the absence of non-content messages. In addition to generalizing [16] to scenarios with both content and non-content traffic, our work improves upon this previous result in several ways. First, our new converse leads to a tighter order optimality result, reducing the multiplicative factor obtained in [16] from 4.02 to 2.01. Second, our result extends the achievability argument in [16] to the case with non-integer normalized aggregate cache size $K\mu$, and the case with more users than files (i.e. $N < K$). We show that for non integer $K\mu$, a direct application of the memory-sharing principle yields a strictly suboptimal GNDT, and a superior performance is achieved by treating the physical-layer transmission problem as one with two nested sets of multicast messages. To address the case of $N < K$, we base our achievability on the Yu, Maddah-Ali and Avestimehr (YMA) scheme [5, 6], in contrast to the MN scheme adopted in [16]. Third, we take a few steps beyond [16], and refine and relax the GNDT-GDoF results to obtain approximate delay-rate characterizations, which hold at all finite SNR values.

Another set of closely related results for the cache-aided degraded GBC, in the absence of non-content messages, are found in [10–12], where the exact delay measure (or its rate reciprocal) is considered instead of the GNDT approximation. In [10], the authors focus on minimizing the transmit power subject to a delay constraint—a dual to the more common problem of delay minimization subject to a transmit power constraint. The scheme in [10] can be seen as a special case of the scheme we propose here, after eliminating uncacheable non-content messages, and the derived achievable performance has the merit of exactness. Nevertheless, the achievable delay characterization in [10] highly depends on auxiliary power allocation variables that require further optimization, rendering it less flexible for direct analysis compared to the GNDT characterization we obtain here—see (4) and (7). Moreover, the outer bound in [10] is restricted to uncoded placement schemes and there are no guarantees of order optimality (examined numerically in [10]).

In [11], a setting with multi-layered content is studied, where each file is described by several independent layers representing refinements of the same content (e.g. higher quality), and which are communicated opportunistically depending on users' SNRs. This multi-layered setting shares an important aspect with the mixed traffic setting we study here, i.e. the opportunity to exploit *topological holes* to communicate additional (asymmetric) messages beyond (symmetric) content files. On the other hand, there are also key discrepancies, including the assumption that all file

layers are cacheable, and the dependency of caching schemes on the wireless network topology in [11]. Moreover, the results in [11] inherit some of the limitations in [10], e.g. the inexplicit characterizations which are strongly coupled with auxiliary optimization variables, as well as the lack of information-theoretic optimality guarantees. Finally, in [12] the authors obtain a complete characterization of the optimal delay in the 2-user cache-aided GBC under the restriction of uncoded caching schemes. Nevertheless, it is not yet clear whether the techniques can be extended to more general setting, with an arbitrary number of users and (possibly) coded cache placement.

1.6 Notation

For positive integers z_1 and z_2 , with $z_1 \leq z_2$, the sets $\{1, 2, \dots, z_1\}$ and $\{z_1, z_1 + 1, \dots, z_2\}$ are denoted by $[z_1]$ and $[z_1 : z_2]$, respectively. $\binom{z_2}{z_1}$ denotes the binomial coefficient. For a real number a , we denote $\max\{0, a\}$ by $(a)^+$. The tuple $(a_1, \dots, a_y, b_1, \dots, b_z)$ is denoted by $(a_i : i \in [y], b_i : i \in [z])$. The cardinality of set \mathcal{A} is denoted by $|\mathcal{A}|$. For sets \mathcal{A} and \mathcal{B} , the set of elements in \mathcal{A} and not in \mathcal{B} is denoted by $\mathcal{A} \setminus \mathcal{B}$. For any $\mathcal{A} \subseteq \mathbb{R}^K$, the closure of set \mathcal{A} is denoted by $\text{cl}\{\mathcal{A}\}$.

2 Problem Setting

In this section, we formally describe the system model introduced in Section 1.3, and then proceed to define the performance measures and formulate the problem. As mentioned earlier, we consider wireless network consisting of a single transmitter (server) and K receivers (users). The transmitter has access to a content library of N files, denoted by F_1, \dots, F_N , each of size B bits. Each user k is equipped with an isolated cache memory of size MB bits, where $M \in [0, N]$. The network operates in two phases: a *placement phase* and a *delivery phase*.

1. *Placement phase*: During this phase, users have access to the entire library of files to fill the content of their caches. This occurs without knowledge of future file requests.
2. *Delivery phase*: Each user k requests a *content* file F_{d_k} , where $d_k \in [N]$ is the corresponding demand index. Moreover, the transmitter generates K *non-content* messages W_1, \dots, W_K , intended to users $1, \dots, K$, respectively. These messages are mutually independent, independent of the content library, and may vary in size. During the delivery phase, the transmitter sends a codeword over the physical channel; while each user k receives a corresponding noisy signal and tries to recover (F_{d_k}, W_k) from this signal and the local cache content.

Remark 1. (Files and Messages). The word “*files*” is used to describe F_1, \dots, F_N , which are pre-generated *content* messages, known beforehand to the server and revealed to users during the placement phase. Files represent predictable types of traffic, e.g. popular internet content. On the other hand, the word “*messages*” describes W_1, \dots, W_K , which are classical *non-content* messages generated in real time just ahead of transmission during the delivery phase. Messages represent unpredictable types of traffic, e.g. voice and video calls, or recent internet content.

2.1 Physical channel

The physical channel is a K -user degraded GBC. In the t -th use of the physical channel, where $t \in \mathbb{N}$, the input-output relationship is described as:

$$Y_k(t) = h_k X(t) + Z_k(t). \quad (8)$$

In the above, $X(t) \in \mathbb{C}$ is the input signal; while $Y_k(t), Z_k(t), h_k \in \mathbb{C}$ are the output signal, zero-mean, unit-variance additive white Gaussian noise (AWGN) signal, and the (fixed) channel coefficient of user k , respectively. Communication occurs over T channel uses, in which the transmitter is subject to a unit average power constraint given by

$$\frac{1}{T} \sum_{t=1}^T |X(t)|^2 \leq 1. \quad (9)$$

For each user k , the SNR is controlled by the corresponding channel coefficient, and is given by $\text{SNR}_k = |h_k|^2$. We assume, without loss of generality, that the following order holds:

$$\text{SNR}_1 \leq \text{SNR}_2 \leq \dots \leq \text{SNR}_K. \quad (10)$$

For GDoF (and GNDT) purposes, we express the SNR of each user k as

$$\text{SNR}_k = P^{\alpha_k} \quad (11)$$

where the exponent α_k is known as the *channel strength level*, while $P > 1$ is a *nominal power parameter* which approaches infinity to define the GDoF limit—see [22, 39–41]. We assume without loss of generality that $\alpha_k \in (0, 1]$ and $\alpha_K = 1$, which alongside the order in (10) translate to

$$0 < \alpha_1 \leq \alpha_2 \leq \dots \leq \alpha_K = 1. \quad (12)$$

The channel strength tuple is given by $\boldsymbol{\alpha} \triangleq (\alpha_1, \dots, \alpha_K)$.

Remark 2. Truncating channel strength levels such that $\alpha_k > 0$ translates to $\text{SNR}_k > 1$ for all users $k \in [K]$ (recall that $P > 1$), which is common practice in GDoF studies. This excludes scenarios where $\text{SNR}_i \leq 1$ for some users $i \in [K]$, as such users receive their desired signals at the same level of noise (at best), and hence achieve zero GDoF. In the constant-gap capacity sense, $\text{SNR}_i \leq 1$ leads to an achievable rate which is bounded above by 1 bit per channel use. Therefore, an achievable rate region which excludes user i , e.g. by setting the corresponding rate to zero, may still be within 1 bit per channel use from the capacity region.

2.2 Codes, Rates and Delay

Files F_1, \dots, F_N are independent random variables, each uniformly distributed over the set $[2^{\lfloor B \rfloor}]$. To define asymptotic limits, we scale the file size B with the number of physical channel uses T as $B = TR_F$, where R_F is the content rate in bits per channel use. Messages W_1, \dots, W_K are also independent random variables, yet not necessarily identical. Each W_k is uniformly distributed over the set $[2^{\lfloor TR_k \rfloor}]$, where R_k is the corresponding message rate and $\mathbf{R} \triangleq (R_1, \dots, R_K)$ denotes a message rate tuple. A demand tuple is defined as $\mathbf{d} \triangleq (d_1, \dots, d_K) \in [N]^K$.

A code (T, R_F, \mathbf{R}, M) consists of the above file and message sets in addition to the following:

- A caching strategy $\boldsymbol{\phi} \triangleq (\phi_1, \dots, \phi_K)$, comprising K caching functions. Each caching function $\phi_k : [2^{\lfloor TR_F \rfloor}]^N \rightarrow [2^{\lfloor TR_F M \rfloor}]$ is a map between the N library files and the cache content of the corresponding user k , denoted by U_k . That is

$$U_k = \phi_k(F_1, \dots, F_N). \quad (13)$$

- An encoding function $\psi : [N]^K \times [2^{\lfloor TR_F \rfloor}]^N \times [2^{\lfloor TR_1 \rfloor}] \times \dots \times [2^{\lfloor TR_K \rfloor}] \rightarrow \mathbb{C}^T$ which maps the demand tuple, N files and K messages to a codeword $X^T \triangleq (X(1), \dots, X(T))$, which satisfies the power constraint in (9). In particular, we have

$$X^T = \psi(\mathbf{d}, F_1, \dots, F_N, W_1, \dots, W_K). \quad (14)$$

- A decoding strategy $\boldsymbol{\eta} \triangleq (\eta_1, \dots, \eta_K)$, comprising K decoding functions. Each decoding function $\eta_k : [N]^K \times \mathbb{C}^T \times [2^{\lfloor TR_F M \rfloor}] \rightarrow [2^{\lfloor TR_F \rfloor}] \times [2^{\lfloor TR_k \rfloor}]$ maps the demand tuple, received signal $Y_k^T \triangleq (Y_k(1), \dots, Y_k(T))$ and local cache content to an estimate of (F_{d_k}, W_k) , i.e.

$$(\hat{F}_{d_k}, \hat{W}_k) = \eta_k(\mathbf{d}, Y_k^T, U_k). \quad (15)$$

For any code (T, R_F, \mathbf{R}, M) , the probability of decoding error is defined as

$$P_{e,T} \triangleq \max_{\mathbf{d} \in [N]^K} \max_{k \in [K]} \Pr \left\{ (\hat{F}_{d_k}, \hat{W}_k) \neq (F_{d_k}, W_k) \right\} \quad (16)$$

which accounts for the worst-case file demand tuple amongst all N^K possible user demands.

It is instructive to work with the reciprocal of the content rate R_F , which enjoys desirable analytical properties, see, e.g., [27, 31]. To this end, we define

$$\mathcal{T} \triangleq \frac{1}{R_F} = \frac{T}{B} \quad (17)$$

which is the number of physical channel uses required to communicate one bit of content to each user. Since channel uses often correspond to time instance, \mathcal{T} is referred to as the *delivery time* or *delay*, used interchangeably. Given a memory size M , a delay-rate trade-off is denoted by the tuple $(\mathcal{T}, \mathbf{R}; M)$, which is achievable if there exists a sequence of $(T, 1/T, \mathbf{R}, M)$ codes such that $P_{e,T} \rightarrow 0$ as $T \rightarrow \infty$. For any $(\mathbf{R}; M)$, the optimal (content) delivery time is defined as:⁴

$$\mathcal{T}^*(\mathbf{R}; M) \triangleq \inf \{ \mathcal{T} : (\mathcal{T}, \mathbf{R}; M) \text{ is achievable} \}. \quad (18)$$

Conversely, for any $(\mathcal{T}; M)$, the (non-content) capacity region is defined as:

$$\mathcal{C}(\mathcal{T}; M) \triangleq \text{cl} \{ \mathbf{R} : (\mathcal{T}, \mathbf{R}; M) \text{ is achievable} \}. \quad (19)$$

Remark 3. (Worst-case demands). We adopt a worst-case definition of performance measures (e.g. delay and capacity region) with respect to user demands—see the decoding error probability in (16). Therefore, without loss of generality, we assume henceforth that demand tuples \mathbf{d} comprise $\min\{K, N\}$ distinct user demands. Moreover, in scenarios where $N < K$, worst-case demands occur when the first (i.e. weakest) N users make distinct file demands, as we will see further on in Section 5. A similar observation regarding the form of worst-case demand tuples when $N < K$ was made in [10], where the focus is on minimizing the transmit power subject to a constraint on R_F (or \mathcal{T}) in the cache-aided degraded GBC, in the absence of non-content messages.

2.3 GDoF and GNDT

In defining the GDoF and GNDT limits, the dependency of the rates and delivery time on P is highlighted. That is, for any given M and P , an achievable delay-rate tuple is denoted by $(\mathcal{T}(P), \mathbf{R}(P); M)$, while $\mathcal{T}^*(\mathbf{R}; M, P)$ and $\mathcal{C}(\mathcal{T}; M, P)$ describe the optimal trade-offs.

We denote a GDoF tuple by $\mathbf{r} \triangleq (r_1, \dots, r_K)$, where r_k is the GDoF of user k , while the GNDT is denoted by τ . For given M , a GNDT-GDoF trade-off $(\tau, \mathbf{r}; M)$ is achievable if there exists a sequence of achievable delay-rate tuples $(\mathcal{T}(P), \mathbf{R}(P); M)$, for all P , such that

$$r_k = \lim_{P \rightarrow \infty} \frac{R_k(P)}{\log(1 + P)}, \quad \forall k \in [K] \quad (20)$$

⁴When describing a trade-off of performance measures, e.g. $\mathcal{C}(\mathcal{T}; M)$, a semicolon separates performance measure arguments (e.g. \mathcal{T}) from arguments representing fixed system parameters (e.g. M).

$$\tau = \lim_{P \rightarrow \infty} \mathcal{T}(P) \log(1 + P). \quad (21)$$

For any $(\mathbf{r}; M)$, the optimal GNDT is defined as

$$\tau^*(\mathbf{r}; M) \triangleq \inf \{ \tau : (\tau, \mathbf{r}; M) \text{ is achievable} \}. \quad (22)$$

On other hand, for any pair $(\tau; M)$, the optimal GDoF region is defined as:

$$\mathcal{D}(\tau; M) = \text{cl} \{ \mathbf{r} : (\tau, \mathbf{r}; M) \text{ is achievable} \}. \quad (23)$$

Remark 4. (Time slots). We measure the GNDT in *time slots*, where 1 time slot corresponds to the overall delay of delivering a single file to the strongest user (i.e. user K) in the absence of caches, interference and instantaneous messages, as P approaches infinity. In this isolated single-user scenario, the delivery time (per bit) is given by $\mathcal{T}_0(P) = 1/\log(1 + P)$, and the overall delay is given by $B\mathcal{T}_0(P) = B/\log(1 + P)$ in channel uses. Now suppose that in a general setting with arbitrary number users and cache sizes, we deliver a file of size B to each user with delay $\mathcal{T}(P)$. The corresponding GNDT is given by

$$\tau \triangleq \lim_{P \rightarrow \infty} \mathcal{T}(P) \log(1 + P) = \lim_{P \rightarrow \infty} \frac{B\mathcal{T}(P)}{B\mathcal{T}_0(P)}. \quad (24)$$

The ratio in (24) makes the definition of the GNDT and its time slot unit all the more clear.

Remark 5. The delay, capacity, GNDT and GDoF characterizations we obtain in this work all depend on the normalized memory size μ instead of the actual memory size M . This is reflected in the arguments of the performance measures in the following sections, where μ replaces M . Moreover, we highlight the dependency on the channel strength levels, e.g. $\tau^*(\mathbf{r}; \mu, \boldsymbol{\alpha})$ and $\mathcal{D}(\tau; \mu, \boldsymbol{\alpha})$, and the nominal power parameter, e.g. $\mathcal{C}(\mathcal{T}; \mu, \boldsymbol{\alpha}, P)$ and $\mathcal{T}^*(\mathbf{R}; \mu, \boldsymbol{\alpha}, P)$.

3 Main Result and Insights

We start this section by defining an upper bound for the GNDT given any GDoF tuple \mathbf{r} .

Definition 1. For any $\mu, \boldsymbol{\alpha}$ and \mathbf{r} , we define⁵

$$\tau^{\text{ub}}(\mathbf{r}; \mu, \boldsymbol{\alpha}) \triangleq \max_{k \in [K]} \left\{ \frac{1}{(\alpha_k - \sum_{i \in [k]} r_i)^+} \cdot \text{conv} \left(\frac{\binom{K}{K\mu+1} - \binom{K - \min\{k, N\}}{K\mu+1}}{\binom{K}{K\mu}} \right) \right\} \quad (25)$$

where $\text{conv}(f(K\mu))$ denotes the lower convex envelope of the points $\{(K\mu, f(K\mu)) : K\mu \in [0 : K]\}$.

Equipped with Definition 1, we are now ready to present the main theorem of this work.

Theorem 1. *The GNDT-GDoF trade-off described by $\tau^{\text{ub}}(\mathbf{r}; \mu, \boldsymbol{\alpha})$ in (25) is achievable. Moreover, $\tau^{\text{ub}}(\mathbf{r}; \mu, \boldsymbol{\alpha})$ is within a multiplicative factor of 2.01 from the optimal trade-off, that is⁶*

$$\frac{1}{2.01} \cdot \tau^{\text{ub}}(\mathbf{r}; \mu, \boldsymbol{\alpha}) \leq \tau^*(\mathbf{r}; \mu, \boldsymbol{\alpha}) \leq \tau^{\text{ub}}(\mathbf{r}; \mu, \boldsymbol{\alpha}). \quad (26)$$

The achievability of Theorem 1 is presented in Sections 4 and 5, with some details relegated to Appendix A. For ease of exposition, the focus of these sections is on integer values of $K\mu$, while the extension to non-integer $K\mu$ is relegated to Appendix B. On the other hand, the converse of Theorem 1 is presented in Section 6. Next, we draw some insights from the main result. We start by focusing on integer $K\mu$, and then discuss the case with non-integer $K\mu$ further on.

⁵In (25), and throughout this work, we use the convention $\binom{n}{k} = 0$, for all $n < k$.

⁶The multiplicative factor is in fact 2.00884, which is consistent with the result of Yu et al. [6].

3.1 Separation principle

The achievability of $\tau^{\text{ub}}(\mathbf{r}; \mu, \boldsymbol{\alpha})$ employs a separation-based strategy, which isolates the content caching and delivery problem from the physical-layer transmission problem. In particular, caching, generating coded multicast messages (XORs), and recovering demanded files from received multicast messages and local cache contents are all carried out at the bit level in the noiseless shared link manner [3, 5, 6], and are oblivious to the transmission strategy over the physical channel. On the other hand, the physical channel sees $\binom{K}{K\mu+1}$ multicast messages (coded content) and K unicast messages (non-content), and communicates them in a joint multicast and unicast fashion.

The physical-layer scheme employs power control with superposition coding and successive decoding. Hence different GNDT-GDoF trade-offs, described by the relationship in (25), are achieved by tuning the underlying power allocation and GDoF assignment problems. A detailed exposition of the physical-layer scheme is given in Section 4 (see also Appendix A).

3.2 GNDT in the absence of non-content messages

As a special case of Theorem 1, we recover the achievability result in [16], where it was shown that for $N \geq K$ and integer $K\mu$, and in the absence of non-content messages, one can achieve

$$\tau^{\text{ub}}(\mathbf{0}; \mu, \boldsymbol{\alpha}) = \max_{k \in [K]} \left\{ \frac{1}{\alpha_k} \cdot \frac{\binom{K}{K\mu+1} - \binom{K-k}{K\mu+1}}{\binom{K}{K\mu}} \right\}. \quad (27)$$

The order optimality of $\tau^{\text{ub}}(\mathbf{0}; \mu, \boldsymbol{\alpha})$ up to a multiplicative factor of 4.02 is also proved in [16], which we tighten in Theorem 1 by a factor of 2. Moreover, in addition to strengthening the order optimality result, our new achievability proof (given in Sections 4 and 5) sheds new light on the achievable GNDT in (27), and provides an operational interpretation in terms of the multiple multicast GDoF region of the underlying degraded GBC.

To illustrate, consider a setting with $K = N = 3$ and $M = 1$, and assume that each user requests a distinct file. Employing a separation-based strategy, a standard coded caching scheme delivers 3 coded multicast messages: W_{12} , W_{13} and W_{23} , each designated to a pair of users specified by the message index; and each of size $1/3$ in (normalized) file units. On the other hand, the physical channel communicates the coded messages in a multiple multicast fashion and, as shown in Theorem 2 in Section 4, operates at any non-negative GDoF tuple (r_{12}, r_{13}, r_{23}) that satisfies⁷

$$\begin{aligned} r_{12} + r_{13} &\leq \alpha_1 \\ r_{12} + r_{13} + r_{23} &\leq \alpha_2. \end{aligned} \quad (28)$$

The GDoF region in (28) admits an intuitive interpretation. User 1 recovers both W_{12} and W_{13} , and hence the sum-GDoF of these messages is bounded by the channel strength α_1 . Due to the degradedness of the physical channel, user 2 can decode whatever user 1 decodes, and must additionally recover W_{23} . Therefore, the total GDoF cannot exceed α_2 . It is clear that user 3, i.e. the strongest user, can recover all messages as $\alpha_2 \leq \alpha_3$. Since all 3 coded messages are of equal size, it is most efficient to operate at the symmetric multicast GDoF $r_{\text{sym}} = \min \left\{ \frac{\alpha_1}{2}, \frac{\alpha_2}{3} \right\}$, which is directly computed from (28)—see Fig. 2. The achievable GNDT is hence given by

$$\tau = \frac{1}{3} \cdot \frac{1}{r_{\text{sym}}} \quad (29)$$

which exactly coincides with (27) for $K = 3$ and $\mu = 1/3$. As it turns out, the same argument

⁷Note that the multicast GDoF tuple here should not be confused with the non-content GDoF tuple \mathbf{r} . This will be further clarified in Section 4.

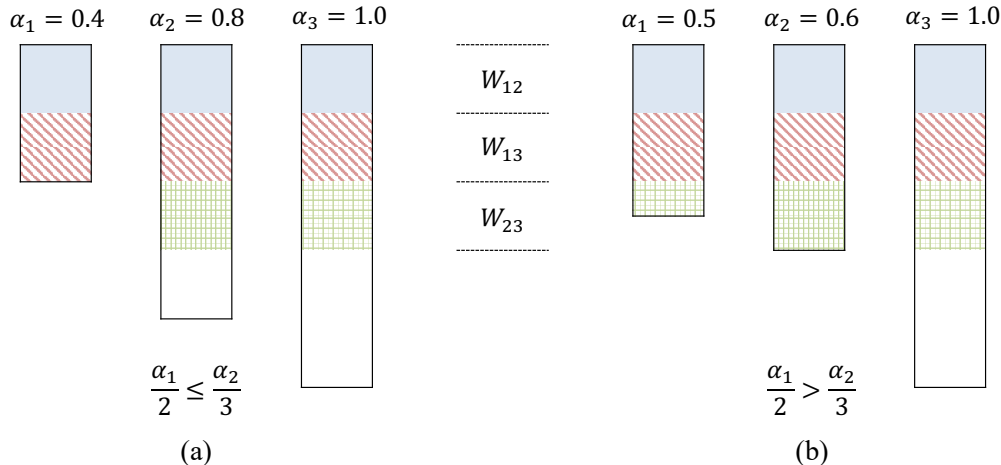


Figure 2: Received signal power levels in a 3-user degraded GBC with multiple multicast messages, where W_{ij} is intended to users i and j (group size of 2), and a symmetric GDoF of $r_{\text{sym}} = 0.2$ is achieved in both (a) and (b). Top levels represent signals transmitted with higher powers, received by all users above their respective noise levels (bottom end of each bar). Bottom levels represent signals transmitted with lower powers, heard by sufficiently strong users and corrupted by noise (hence clipped) at weaker users. Multicast messages (coloured levels) can carry coded content (e.g. $\mu = 1/3$). Uncoloured signal levels (in white) are unoccupied, representing *topological holes* for communicating non-content messages (see Corollary 1).

extends to general settings, where the achievable GNDT in (27) is decomposed as

$$\tau^{\text{ub}}(\mathbf{0}; \mu, \boldsymbol{\alpha}) = \underbrace{\frac{1}{\binom{K}{K\mu}}}_{\text{norm. size}} \cdot \underbrace{\max_{k \in [K-K\mu]} \left\{ \frac{\binom{K}{K\mu+1} - \binom{K-k}{K\mu+1}}{\alpha_k} \right\}}_{1/r_{\text{sym}}}. \quad (30)$$

The first term on the right-hand-side of (30) is the normalized size of each coded multicast message; while the second term is the reciprocal of the symmetric multiple multicast GDoF, derived from the multiple multicast GDoF region of the underlying GBC (see Corollary 3, Section 4.2).

3.3 Achievable GDoF under minimum GNDT

Let us now plug non-content messages back in, while maintaining the assumption that $N \geq K$ for ease of exposition. Theorem 1 suggests that in scenarios with asymmetric channel strengths, the order-optimal GNDT in (27), achieved by eliminating non-content messages, can be maintained while simultaneously achieving non-zero GDoF for (some) non-content messages. To see this, let us define user k^* (*bottleneck user* in [16]) such that

$$k^* \triangleq \arg \max_{k \in [K]} \left\{ \frac{\binom{K}{K\mu+1} - \binom{K-k}{K\mu+1}}{\alpha_k} \right\} \quad (31)$$

For example, in the illustrations shown in Fig. 2, with $K = 3$ and $K\mu + 1 = 2$, we have $k^* = 1$ in (a), where $\frac{\alpha_1}{2} \leq \frac{\alpha_2}{3}$; and $k^* = 2$ in (b), where $\frac{\alpha_1}{2} > \frac{\alpha_2}{3}$. In terms of the multiple multicast GDoF region of the underlying GBC, k^* is the (smallest) index such that the inequality that delimits the sum-GDoF of messages decoded by user k^* holds with equality (see Theorem 2).

From (25), it follows that achieving a GNDT of $\tau^{\text{ub}}(\mathbf{0}; \mu, \boldsymbol{\alpha})$ through the proposed strategy requires setting $r_k = 0$, for all $k \in [k^*]$. That is, we cannot send additional information to

the bottleneck user k^* , or weaker users whose messages are also decodable by user k^* , without increasing the achievable GNDT. However, users in $[k^* + 1 : K]$ can achieve non-zero non-content GDoF without affecting the GNDT in (27), by communicating through the *topological holes* arising from the asymmetry in channel strength levels, specifically when $\alpha_{k^*} < \alpha_{k^*+1}$. These achievable non-content GDoF tuples are described as follows.

Corollary 1. (Topological Holes). A minimum GNDT of $\tau^{\text{ub}}(\mathbf{r}; \mu, \boldsymbol{\alpha}) = \tau^{\text{ub}}(\mathbf{0}; \mu, \boldsymbol{\alpha})$ and a non-content GDoF tuple \mathbf{r} are simultaneously achievable given that the GDoF tuple $\mathbf{r} \in \mathbb{R}_+^K$ satisfies

$$r_k = 0, \forall k \in [k^*]$$

$$r_{k^*+1} + \dots + r_k \leq \alpha_{k^*+1} - \alpha_{k^*} \cdot \left(\frac{\binom{K}{K\mu+1} - \binom{K-k}{K\mu+1}}{\binom{K}{K\mu+1} - \binom{K-k^*}{K\mu+1}} \right), \forall k \in [k^* + 1 : K]. \quad (32)$$

Examples that illustrate Corollary 1 using signal power levels, measured in terms of the exponent of P (see, e.g., [40, 41]), are shown in Fig. 2. As argued in Section 1.3, the current treatment of content traffic and non-content traffic as two independent entities leads to scheduling the two types of traffic on orthogonal wireless resource blocks, which is suboptimal in general. This observation is made concrete in the following remark by leveraging Corollary 1.

Remark 6. Suppose that we wish to deliver content at the minimum achievable GNDT given by $\tau = \tau^{\text{ub}}(\mathbf{0}; \mu, \boldsymbol{\alpha})$. From Corollary 1, we know that we can simultaneously communicate a non-content message to, e.g., user K with a GDoF of r_K , which satisfies the corresponding inequality in (32); hence delivering additional non-content information of $\tau \cdot r_K$ in normalized file units.⁸ An alternative approach is to deliver content traffic and non-content traffic over orthogonal resource blocks using, e.g., time-sharing (see Section 1.3). This incurs an additional delay of at least $\tau \cdot r_K / \alpha_K$ time slots, required to deliver the same amount of non-content information separately. For the examples shown in Fig. 2, this corresponds to an increase of 40% in communication delay.

3.4 Non-integer $K\mu$

Using the separation-based strategy described above, a GNDT-GDoF trade-off of $\tau^{\text{ub}}(\mathbf{r}; \mu, \boldsymbol{\alpha})$ is achieved for all μ such that $K\mu$ is an integer. In this case, the $\text{conv}(\cdot)$ operator in (25) is dropped and the corresponding achievable GNDT can be expressed by

$$\tau_{K\mu \in \mathbb{Z}}^{\text{ub}}(\mathbf{r}; \mu, \boldsymbol{\alpha}) \triangleq \max_{k \in [K]} \left\{ \frac{1}{(\alpha_k - \sum_{i \in [k]} r_i)^+} \cdot \frac{\binom{K}{K\mu+1} - \binom{K - \min\{k, N\}}{K\mu+1}}{\binom{K}{K\mu}} \right\}. \quad (33)$$

For μ such that $K\mu$ takes non-integer values drawn from $(0, K)$, a standard memory-sharing argument [3] achieves the lower convex envelope of the points in (33), defined as

$$\tau_{\text{ms}}^{\text{ub}}(\mathbf{r}; \mu, \boldsymbol{\alpha}) \triangleq \text{conv} \left(\max_{k \in [K]} \left\{ \frac{1}{(\alpha_k - \sum_{i \in [k]} r_i)^+} \cdot \frac{\binom{K}{K\mu+1} - \binom{K - \min\{k, N\}}{K\mu+1}}{\binom{K}{K\mu}} \right\} \right). \quad (34)$$

In this straightforward application of the memory-sharing principle, files, caches and transmissions are divided proportionally such that the system effectively operates as two systems: one with a multicasting gain of $\lfloor K\mu + 1 \rfloor$, and another with a multicasting gain of $\lceil K\mu + 1 \rceil$. Nevertheless, it turns out that this strategy can be strictly improved upon, especially in asymmetric settings.

⁸Recall from Remark 4 that τ , in times slots, is measured per file delivered over a channel with a GDoF of 1. Therefore, $\tau \cdot r_K$ corresponds to delivered information in file units.

In the improved strategy, caching and preparing the sets of coded multicast messages are carried out as in the standard memory-sharing scheme. Nevertheless, instead of carrying out the physical-layer transmission *sequentially* in two phases, the degraded GBC *jointly* delivers two sets of coded multicast messages, one with messages intended to $\lfloor K\mu + 1 \rfloor$ users each and another with messages intended to $\lceil K\mu + 1 \rceil$ users each; as well as the non-content unicast message set.⁹ This joint delivery strategy achieves the GNDT in (25), which satisfies

$$\tau^{\text{ub}}(\mathbf{r}; \mu, \boldsymbol{\alpha}) \leq \tau_{\text{ms}}^{\text{ub}}(\mathbf{r}; \mu, \boldsymbol{\alpha}). \quad (35)$$

The inequality in (35) is strict in asymmetric scenarios at some values of μ , as seen through the example in Fig. 3. Details and derivations related to this part can be found in Appendix B.

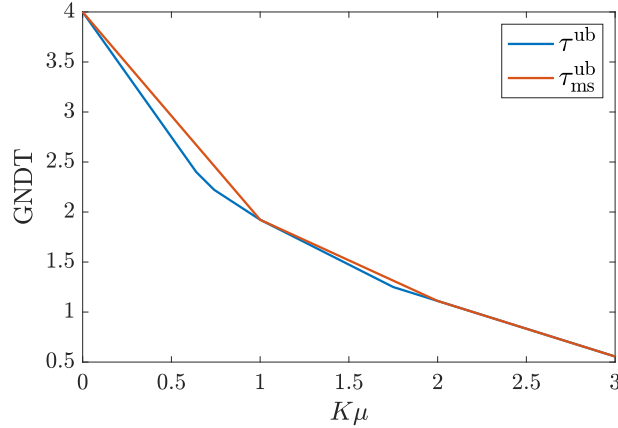


Figure 3: GNDT-memory trade-off curves for $K = N = 4$, $\boldsymbol{\alpha} = (0.45, 0.65, 0.85, 1)$ and $\mathbf{r} = \mathbf{0}$.

Remark 7. The inequality in (35) is another manifestation of the fact that in the degraded GBC, superposition coding is in general superior to time-sharing. A naive application of the memory-sharing principle leads to delivering the two sets of coded multicast messages sequentially in a time shared fashion. While this incurs no loss in symmetric settings (as in, e.g., [3]), it can be strictly suboptimal in non-symmetric settings. On the other hand, the scheme described in Appendix B takes advantage of asymmetry in the degraded GBC through superposition coding.

3.5 GDoF region and delay-rate trade-off

Theorem 1 leads to a characterization of the GDoF region $\mathcal{D}(\tau; \mu, \boldsymbol{\alpha})$, given as follows.

Corollary 2. For any μ , $\boldsymbol{\alpha}$ and τ , the GDoF region $\mathcal{D}(\tau; \mu, \boldsymbol{\alpha})$ satisfies:

$$\mathcal{D}_{\text{in}}(\tau; \mu, \boldsymbol{\alpha}) \subseteq \mathcal{D}(\tau; \mu, \boldsymbol{\alpha}) \subseteq \mathcal{D}_{\text{in}}(2.01 \cdot \tau; \mu, \boldsymbol{\alpha}) \quad (36)$$

where $\mathcal{D}_{\text{in}}(\tau; \mu, \boldsymbol{\alpha})$ as the set of all non-content GDoF tuples $\mathbf{r} \in \mathbb{R}_+^K$ satisfying

$$\sum_{i \in [k]} r_i + \frac{1}{\tau} \cdot \text{conv} \left(\frac{\binom{K}{K\mu+1} - \binom{K - \min\{k, N\}}{K\mu+1}}{\binom{K}{K\mu}} \right) \leq \alpha_k, \quad \forall k \in [K]. \quad (37)$$

⁹The scheme in [10] (implicitly) adopts a similar superposition strategy with two sets of multicast messages.

The achievable GDoF region in Corollary 1 is a special case of the one in Corollary 2—the former is recovered by setting $\tau = \tau^{\text{ub}}(\mathbf{0}; \mu, \boldsymbol{\alpha})$ in $\mathcal{D}_{\text{in}}(\tau; \mu, \boldsymbol{\alpha})$, while restricting to $N \geq K$. We conclude this section with the following remark on characterizing the optimal delay-rate trade-off.

Remark 8. (Approximate delay-rate characterization). As one would hope, the GNDT-GDoF-based characterizations presented in this section translate to counterpart approximate delay-rate characterizations. This is shown in Appendix D, where we characterize the set of all achievable delay-rate trade-off tuples $(\mathcal{T}, \mathbf{R}; \mu)$ up to an additive gap of 2 bits per channel use for rates and a multiplicative gap of 2.01 for the delay, irrespective of all system parameters.

4 Degraded GBC with Unicast and Multiple Multicast Messages

In this section, we focus on a variant of the degraded GBC in Section 2.1 with no caches and with two message sets: a unicast message set and a multiple multicast message set. The latter message set is referred to as the σ -multicast message set, where $\sigma \in [2 : K]$ is the size of the corresponding multicast groups.¹⁰ As seen in the following section, this channel model is at the heart of the separation architecture—unicast messages carry instantaneous non-content traffic (i.e. messages), while σ -multicast messages carry coded content traffic (i.e. files).

4.1 Unicast and σ -multicast message sets

The unicast message set is given by $\{W_k : k \in [K]\}$, where each message W_k is intended to the corresponding user k and has a rate of R_k and a GDoF of r_k ; while σ -multicast message set is given by $\{W_{\mathcal{S}} : \mathcal{S} \subseteq [K], |\mathcal{S}| = \sigma\}$, with each message $W_{\mathcal{S}}$ intended to all users in \mathcal{S} and has a rate of $R_{\mathcal{S}}$ and a GDoF of $r_{\mathcal{S}}$. Note that since $\sigma \geq 2$, there is no ambiguity between W_k and $W_{\mathcal{S}}$, R_k and $R_{\mathcal{S}}$, or r_k and $r_{\mathcal{S}}$, for any $k \in [K]$ and $\mathcal{S} \subseteq [K]$.

For any σ , $\boldsymbol{\alpha}$ and P , the capacity region and GDoF region of the above channel are denoted by $\mathcal{C}^{\text{PHY}}(\sigma, \boldsymbol{\alpha}, P)$ and $\mathcal{D}^{\text{PHY}}(\sigma, \boldsymbol{\alpha})$, respectively. We defined the set of all σ -multicast groups as $\Sigma \triangleq \{\mathcal{S} \subseteq [K] : |\mathcal{S}| = \sigma\}$, where $|\Sigma| = \binom{K}{\sigma}$. Moreover, we introduce a family of subsets of Σ given by $\{\Sigma_i : i \in [K - \sigma + 1]\}$, where each member $\Sigma_i \subseteq \Sigma$ is defined as:

$$\Sigma_i \triangleq \{\mathcal{S} \in \Sigma : \min\{\mathcal{S}\} = i\}. \quad (38)$$

It can be verified that $\{\Sigma_i : i \in [K - \sigma + 1]\}$ is a partition of Σ , that is:

$$\bigcup_{i \in [K - \sigma + 1]} \Sigma_i = \Sigma \quad \text{and} \quad \Sigma_i \cap \Sigma_j = \emptyset, \quad \forall i \neq j. \quad (39)$$

We are now ready to present a characterization of the GDoF region $\mathcal{D}^{\text{PHY}}(\sigma, \boldsymbol{\alpha})$.

Theorem 2. *For the above described degraded GBC with unicast and σ -multicast messages, the GDoF region $\mathcal{D}^{\text{PHY}}(\sigma, \boldsymbol{\alpha})$ is given by all tuples $(r_k : k \in [K], r_{\mathcal{S}} : \mathcal{S} \in \Sigma) \in \mathbb{R}_+^{K + \binom{K}{\sigma}}$ that satisfy*

$$\begin{aligned} \sum_{i \in [k]} r_i + \sum_{\mathcal{S} \in \cup_{i \in [k]} \Sigma_i} r_{\mathcal{S}} &\leq \alpha_k, \quad \forall k \in [K - \sigma + 1] \\ \sum_{i \in [k]} r_i + \sum_{\mathcal{S} \in \Sigma} r_{\mathcal{S}} &\leq \alpha_k, \quad \forall k \in [K - \sigma + 2 : K]. \end{aligned} \quad (40)$$

¹⁰The case with $\sigma = 1$ is ignored as it reduces to having only a unicast message set.

The GDoF region in Theorem 2 is achieved using a scheme based on power control with superposition coding and successive decoding. The full proof is relegated to Appendix A. Theorem 2 has an intuitive interpretation, which is best seen by laying out the inequalities in (40) as

$$r_1 + \sum_{\mathcal{S} \in \Sigma_1} r_{\mathcal{S}} \leq \alpha_1 \quad (41)$$

$$r_1 + r_2 + \sum_{\mathcal{S} \in \Sigma_1 \cup \Sigma_2} r_{\mathcal{S}} \leq \alpha_2 \quad (42)$$

⋮

$$\sum_{i \in [K-\sigma+1]} r_i + \sum_{\mathcal{S} \in \Sigma} r_{\mathcal{S}} \leq \alpha_{K-\sigma+1} \quad (43)$$

⋮

$$\sum_{i \in [K]} r_i + \sum_{\mathcal{S} \in \Sigma} r_{\mathcal{S}} \leq \alpha_K. \quad (44)$$

User 1 recovers all messages in $\{W_1, W_{\mathcal{S}} : \mathcal{S} \in \Sigma_1\}$, and hence the sum-GDoF of such messages cannot exceed the channel strength of this user, as seen in (41). Due to the degradedness of the channel, user 2 can recover whatever user 1 recovers, and must also decode for messages in $\{W_2, W_{\mathcal{S}} : \mathcal{S} \in \Sigma_2\}$. This bounds the sum-GDoF of messages in $\{W_1, W_2, W_{\mathcal{S}} : \mathcal{S} \in \Sigma_1 \cup \Sigma_2\}$ by the channel strength of user 2, as seen in (42). The same argument applies to all users up to user $K - \sigma + 1$, as seen in (43). Beyond user $K - \sigma + 1$, each user k in $[K - \sigma + 2 : K]$ is capable of recovering all messages in $\{W_1, \dots, W_{k-1}, W_{\mathcal{S}} : \mathcal{S} \in \Sigma\}$, and must additionally decode for message W_k . This yields the sum-GDoF bounds in the second line of (40) (see, e.g., (44)).

Remark 9. We augment the definition of the family of subsets given by $\{\Sigma_i : i \in [K - \sigma + 1]\}$ to include $\{\Sigma_i : i \in [K - \sigma + 2 : K]\}$, where we set $\Sigma_i = \emptyset$, for all $i \in [K - \sigma + 2 : K]$. This allows us to express the inequalities in (40) compactly as

$$\sum_{i \in [k]} r_i + \sum_{\mathcal{S} \in \cup_{i \in [k]} \Sigma_i} r_{\mathcal{S}} \leq \alpha_k, \quad \forall k \in [K]. \quad (45)$$

Moreover, throughout this paper, we use the convention $|\emptyset| = 0$.

Remark 10. The characterization of $\mathcal{D}^{\text{PHY}}(\sigma, \alpha)$ in Theorem 2 leads to a characterization of the capacity region $\mathcal{C}^{\text{PHY}}(\sigma, \alpha, P)$ up to a constant gap. Details are relegated to Appendix A.4. While this constant gap result is of interest in its own right, its main significance to this work is that it lays the ground for establishing the approximate delay-rate characterization in Appendix D.

4.2 Symmetric σ -multicast GDoF

We are interested in scenarios where in addition to unicast messages, we wish to communicate a subset of the σ -multicast messages at a symmetric rate. This is specified as follows.

- For a given parameter $s \in [K]$, we wish to communicate the subset of σ -multicast messages where each message is intended to at least one user in $[s]$.
- For the communicated σ -multicast messages, we wish to achieve a symmetric GDoF of r_{sym} .

From (38), it follows that for any $s \in [K]$, the set of σ -multicast messages of interest is given by

$$\{W_S : \mathcal{S} \in \Sigma, \mathcal{S} \cap [s] \neq \emptyset\} = \{W_S : \mathcal{S} \in \cup_{i \in [s]} \Sigma_i\}. \quad (46)$$

It can be verified that the above set comprises all σ -multicast messages whenever $s \geq K - \sigma + 1$. For this scenario of interest, we define a lower dimensional projection of $\mathcal{D}^{\text{PHY}}(\sigma, \alpha)$ as:

$$\mathcal{D}_{\text{sym}}^{\text{PHY}}(\sigma, \alpha, s) \triangleq \left\{ (r_1, \dots, r_K, r_{\text{sym}}) : (r_k : k \in [K], r_S : \mathcal{S} \in \Sigma) \in \mathcal{D}^{\text{PHY}}(\sigma, \alpha), \right. \\ \left. r_S \geq r_{\text{sym}}, \forall \mathcal{S} \in \cup_{i \in [s]} \Sigma_i, \text{ and } r_S = 0, \forall \mathcal{S} \in \cup_{i \in [s+1:K]} \Sigma_i \right\} \quad (47)$$

which is parametrized by s , in addition to σ and α . A characterization of $\mathcal{D}_{\text{sym}}^{\text{PHY}}(\sigma, \alpha, s)$ is directly obtained from Theorem 2, and is given by all tuples $(r_k : i \in [K], r_{\text{sym}}) \in \mathbb{R}^{K+1}$ that satisfy:

$$\sum_{i \in [k]} r_i + \left| \bigcup_{i \in [\min\{k, s\}]} \Sigma_i \right| \cdot r_{\text{sym}} \leq \alpha_k, \quad \forall k \in [K]. \quad (48)$$

Next, we observe that the following identity holds

$$\left| \bigcup_{i \in [j]} \Sigma_i \right| = \sum_{i \in [j]} |\Sigma_i| = \binom{K}{\sigma} - \binom{K-j}{\sigma}, \quad \forall j \in [K]. \quad (49)$$

This is deduced by noting that $|\Sigma| = \binom{K}{\sigma}$ and $|\cup_{i \in [j+1:K]} \Sigma_i| = \binom{K-j}{\sigma}$, where the latter follows from the fact that $\cup_{i \in [j+1:K]} \Sigma_i$ is the family of all subsets of $[j+1 : K]$ with size σ . Since $|\cup_{i \in [j]} \Sigma_i| = |\Sigma| - |\cup_{i \in [j+1:K]} \Sigma_i|$, the identity in (49) holds. By setting j in (49) to $\min\{k, s\}$ and plugging the identity back into (48), we obtain the following corollary.

Corollary 3. The symmetric σ -multicast GDoF region $\mathcal{D}_{\text{sym}}^{\text{PHY}}(\sigma, \alpha, s)$ is given by all GDoF tuples $(r_k : i \in [K], r_{\text{sym}}) \in \mathbb{R}^{K+1}$ that satisfy:

$$\sum_{i \in [k]} r_i + \left[\binom{K}{\sigma} - \binom{K - \min\{k, s\}}{\sigma} \right] \cdot r_{\text{sym}} \leq \alpha_k, \quad \forall k \in [K]. \quad (50)$$

From the characterization of $\mathcal{D}_{\text{sym}}^{\text{PHY}}(\sigma, \alpha, s)$ in the above corollary, it follows that for any unicast GDoF tuple $(r_k : k \in [K])$, we achieve any symmetric multicast GDoF that satisfies

$$r_{\text{sym}} \leq \min_{k \in [K]} \left\{ \frac{(\alpha_k - \sum_{i \in [k]} r_i)^+}{\binom{K}{\sigma} - \binom{K - \min\{k, s\}}{\sigma}} \right\}. \quad (51)$$

5 Achievability

Equipped with the GDoF characterization for the degraded GBC with unicast and σ -multicast messages derived in the previous section, the achievability part of Theorem 1 will follow from a scheme that adheres to the separation principle, as we will see in this section.

For content placement, generating coded multicast messages, and recovering files from local cache contents and received multicast messages, we invoke the YMA scheme in [5, 6]; which generalizes the original MN scheme [3], and reduces to it whenever $N \geq K$. On the other hand, the physical channel is treated as a collection of capacitated bit pipes, each carrying its corresponding coded multicast message or non-content unicast message, at rates (or GDoF) governed by the characterization in Theorem 2. We focus on integer values of $K\mu$, drawn from $[0 : K]$ in this section. The case of non-integer $K\mu$, drawn from $(0, K)$, is treated in Appendix B.

5.1 Cache placement

Each file F_n is divided into $\binom{K}{K\mu}$ equal sized sub-files, i.e.

$$F_n \rightarrow \left\{ F_n^{\mathcal{S}'} : \mathcal{S}' \subseteq [K], |\mathcal{S}'| = K\mu \right\} \quad (52)$$

where each sub-file $F_n^{\mathcal{S}'}$ has a size of $B/\binom{K}{K\mu}$ bits. Each user k then fills its cache memory as:

$$U_k = \left\{ F_n^{\mathcal{S}'} : n \in [N], \mathcal{S}' \subseteq [K], |\mathcal{S}'| = K\mu, k \in \mathcal{S}' \right\}. \quad (53)$$

This caching strategy satisfies the cache size constraint of MB bits, (see, e.g., [3]). Note that the above-described procedure exactly matches the original MN uncoded caching procedure in [3], which is clearly independent of user demand tuples. We now proceed to describe the coded multicasting and transmission procedures, which depend on the demand tuple type.

5.2 Coded multicast messages

Let us recall from Remark 3 that we consider worst-case demand tuples that comprise of the maximum possible number of distinct user demands, i.e. $\min\{K, N\}$. For ease of exposition, we start by focusing on the case where these distinct demands are made by the first (i.e. weakest) $\min\{K, N\}$ users. In Appendix C, we show that the performance achieved in this case is also achievable whenever the distinct demands are not necessarily made by the weakest users.

We refer to $\mathcal{U} = [\min\{K, N\}]$ as the set of *leading users*, where such users request distinct files, while the set of *non-leading users* is given by $\bar{\mathcal{U}} = [K] \setminus \mathcal{U}$. For brevity, we use the physical channel notation from the previous section and set the multicast group size to $\sigma = K\mu + 1$, and the number of distinct demands to $s = \min\{K, N\}$. Once demands are revealed, the transmitter generates $\binom{K}{\sigma} - \binom{K-s}{\sigma}$ coded multicast messages, each intended to a unique subset of σ users denoted by \mathcal{S} , where $\mathcal{S} \in \cup_{i \in [s]} \Sigma_i$. It can be verified that each such subset of users, i.e. $\mathcal{S} \in \cup_{i \in [s]} \Sigma_i$, contains at least one leading user from $\mathcal{U} = [s]$. The coded multicast message corresponding to \mathcal{S} is given by

$$W_{\mathcal{S}} = \bigoplus_{i \in \mathcal{S}} F_{d_i}^{\mathcal{S} \setminus \{i\}}. \quad (54)$$

Assuming the successful delivery of coded multicast messages, each leading user $k \in \mathcal{U}$ recovers the requested file F_{d_k} from the the set of coded multicast messages $\{W_{\mathcal{S}} : \mathcal{S} \in \cup_{i \in [s]} \Sigma_i, k \in \mathcal{S}\}$ and the cache content U_k , using the standard MN decoding procedure. In particular, each $W_{\mathcal{S}}$ with $k \in \mathcal{S}$ may be expressed as $W_{\{k\} \cup \mathcal{S}'} = F_{d_k}^{\mathcal{S}'} \oplus \left(\bigoplus_{i \in \mathcal{S}'} F_{d_i}^{\{k\} \cup \mathcal{S}' \setminus \{i\}} \right)$, where $\mathcal{S}' = \mathcal{S} \setminus \{k\}$, from which undesired sub-files can be cancelled out, as they are available in U_k . For scenarios where $N \geq K - \sigma + 1$, coded multicast messages corresponding to all subsets of σ users are transmitted, and non-leading users decode their requested files according to the above procedure.

For scenarios where $N \leq K - \sigma$, only a subset of coded multicast messages is transmitted, i.e. those useful to leading users. Nevertheless, non-leading users can also recover their requested files using the YMA decoding procedure [5], subject to the successful decoding of required multicast messages, discussed further on. In particular, a non-leading user $k \in \bar{\mathcal{U}}$ computes the *missing* set coded multicast messages, that is $\{W_{\mathcal{A}} : \mathcal{A} \subseteq \bar{\mathcal{U}}, |\mathcal{A}| = \sigma, k \in \mathcal{A}\}$, from a subset of the transmitted multicast messages and then proceeds to recover F_{d_k} using the standard MN decoding procedure. Each missing message $W_{\mathcal{A}}$ is computed by users in \mathcal{A} as

$$W_{\mathcal{A}} = \bigoplus_{\mathcal{V} \in \Upsilon} W_{\mathcal{B} \setminus \mathcal{V}} \quad (55)$$

where $\mathcal{B} = \mathcal{A} \cup \mathcal{U}$, and Υ denotes a family of subsets of \mathcal{B} such that each member $\mathcal{V} \in \Upsilon$ is a set of N users with distinct demands, and $\mathcal{V} \neq \mathcal{U}$; i.e. each \mathcal{V} is a potential set of leaders other than \mathcal{U} . For more about the YMA procedure, readers are referred to [5, Sec. IV.B].

5.3 Transmission

The problem now reduces to delivering the set of $\binom{K}{\sigma} - \binom{K-s}{\sigma}$ coded multicast messages given by $\{W_{\mathcal{S}} : \mathcal{S} \in \cup_{i \in [s]} \Sigma_i\}$, as well as the set of unicast messages $\{W_k : k \in [K]\}$. This is exactly the unicast and σ -multicast transmission problem discussed in Section 4. Moreover, in scenarios where $N \leq K - \sigma$, the degradedness of the physical channel guarantees that each non-leading user in $\bar{\mathcal{U}} = [N + 1 : K]$ can recover the entire set of multicast messages $\{W_{\mathcal{S}} : \mathcal{S} \in \cup_{i \in [s]} \Sigma_i\}$. This, in turn, ensures the success of the YMA decoding procedure for such users.

Using the symmetric σ -multicast transmission with only a subset of multicast messages in Section 4.2, for any achievable tuple $(\mathbf{r}, r_{\text{sym}}) \in \mathcal{D}_{\text{sym}}^{\text{PHY}}(\sigma, \boldsymbol{\alpha}, s)$, each of the non-content unicast messages achieves its corresponding GDoF in \mathbf{r} , while the achievable content GNDT is given by

$$\tau = \frac{1}{r_{\text{sym}} \cdot \binom{K}{\sigma-1}}. \quad (56)$$

Note that the normalization factor in (56) appears since each coded multicast message $W_{\mathcal{S}}$ has a size of $1/\binom{K}{\sigma-1}$ when normalized by the file size B . Combining with (51), we have

$$\tau \geq \max_{k \in [K]} \left\{ \frac{1}{(\alpha_k - \sum_{i \in [k]} r_i)^+} \cdot \frac{\binom{K}{\sigma} - \binom{K - \min\{k, s\}}{\sigma}}{\binom{K}{\sigma-1}} \right\}. \quad (57)$$

In (57), we have $\min\{k, s\} = \min\{k, \min\{K, N\}\} = \min\{k, N\}$, for all $k \in [K]$. Therefore, (57) coincides with (25), which completes the proof of achievability in this case.

Remark 11. By eliminating non-content messages and restricting to the case of $N \geq K$, the achievability scheme proposed in this paper reduces to the one in [16]. Nevertheless, the proof here is different, specifically the part dealing with transmission over the physical channel. In [16], an explicit power allocation strategy is constructed to achieve the corresponding GNDT. In this paper, we avoid the power allocation problem all together by eliminating the power allocation variables using a Fourier-Motzkin elimination procedure (see Appendix A). This enables us to take the additional step of characterizing the entire GDoF region for the physical channel with unicast and σ -multicast (Section 4), and leads to the GNDT-GDoF trade-off in (57).

6 Converse

In this section, we prove the converse part of Theorem 1. We focus on worst-case demands as defined in Section 5.2. For any such demand tuple \mathbf{d} , each user k in $[K]$ must recover both the message W_k and the demanded file F_{d_k} from the received signal Y_k^T and cache content U_k , with a decoding error that vanishes as T grows large. Therefore, Fano's inequality implies:

$$H(W_k, F_{d_k} | Y_k^T, U_k) \leq 1 + P_{e,T}(TR_k + B) = T\epsilon_T \quad (58)$$

where both $P_{e,T}$ and ϵ_T approach zero as T approaches infinity. Let us now define a side information variable S_k which is independent of W_k . The side information S_k is provided to user k through a genie, and will be specified later on. It follows that

$$TR_k + H(F_{d_k} | U_k, S_k) = H(W_k) + H(F_{d_k} | U_k, S_k)$$

$$\begin{aligned}
&= H(W_k, F_{d_k} | U_k, S_k) \\
&= I(W_k, F_{d_k}; Y_k^T | U_k, S_k) + H(W_k, F_{d_k} | Y_k^T, U_k, S_k) \\
&\leq I(W_k, F_{d_k}; Y_k^T | U_k, S_k) + T\epsilon_T.
\end{aligned} \tag{59}$$

Now let us consider a subset of users $[s]$ with distinct demands, for some $s \in [\min\{K, N\}]$. From the single-user bound in (59), we obtain a multi-user bound for such subset as

$$\sum_{k=1}^s H(F_{d_k} | U_k, S_k) \leq \sum_{k=1}^s \left[I(W_k, F_{d_k}; Y_k^T | U_k, S_k) - T(R_k - \epsilon_T) \right]. \tag{60}$$

Next, we wish to find an upper bound for the right-hand-side of (60), and a lower bound for the left-hand-side of the same inequality. To this end, we apply a symmetrization step over file demands and user orders, which is required to bound below the left-hand-side in (60).

Let $p : [s] \rightarrow [s]$ be a permutation over the subset of users $[s]$, and \mathcal{P}_s be the corresponding set of all $s!$ user permutations. Similarly, $q : [N] \rightarrow [N]$ is a permutation over the set of files $[N]$, and \mathcal{P}_N is the corresponding set of all $N!$ file permutations. For any pair of permutations $(p, q) \in \mathcal{P}_s \times \mathcal{P}_N$, suppose that each user $p(k)$ demands the file $F_{q(k)}$. From (60), we write

$$\sum_{k=1}^s H(F_{q(k)} | U_{p(k)}, S_{p(k)}) \leq \sum_{k=1}^s \left[I(W_{p(k)}, F_{q(k)}; Y_{p(k)}^T | U_{p(k)}, S_{p(k)}) - T(R_{p(k)} - \epsilon_T) \right]. \tag{61}$$

Taking the average of both sides in (61) over all possible permutations $(p, q) \in \mathcal{P}_s \times \mathcal{P}_N$, we obtain

$$\begin{aligned}
\frac{1}{s!N!} \sum_{(p,q) \in \mathcal{P}_s \times \mathcal{P}_N} \sum_{k=1}^s H(F_{q(k)} | U_{p(k)}, S_{p(k)}) &\leq \\
\frac{1}{s!N!} \sum_{(p,q) \in \mathcal{P}_s \times \mathcal{P}_N} \sum_{k=1}^s \left[I(W_{p(k)}, F_{q(k)}; Y_{p(k)}^T | U_{p(k)}, S_{p(k)}) - T(R_{p(k)} - \epsilon_T) \right]. &\tag{62}
\end{aligned}$$

In what follows, we set the side information variable $S_{p(k)}$ for each user $p(k)$ as

$$S_{p(k)} = (W_{p(i)}, F_{q(i)}, U_{p(i)} : i \in [k-1]) \tag{63}$$

consisting of intended messages, demanded files and cache contents of all users that precede user $p(k)$ in the permutation order. Note that the independence between $S_{p(k)}$ and $W_{p(k)}$ is preserved. Moreover, S_{s+1} denotes side information that contains intended messages, demanded files and cache contents of all users in $[s]$. Next, we separately bound each side of the inequality in (62).

6.1 Bounding the right-hand-side of (62)

To this end, we present the following lemma.

Lemma 1. *For any pair of users k and j in $[K]$, such that $k \leq j$, we have*

$$I(W_k, F_{d_k}; Y_k^T | U_k, S_k) \leq I(W_k, F_{d_k}; Y_j^T | U_k, S_k). \tag{64}$$

Proof. The inequality in (64) follows directly from the degradedness of the physical channel. In particular, by considering the physical channel in isolation of the caches, we have the Markov

chain¹¹ $(W_k, F_{d_k}) \rightarrow X^T \rightarrow Y_j^T \rightarrow Y_k^T$. By providing (U_k, S_k) as side information to both users k and j through, this degradedness is not altered, and the following Markov chain holds

$$(W_k, F_{d_k}) \rightarrow (X^T, U_k, S_k) \rightarrow (Y_j^T, U_k, S_k) \rightarrow (Y_k^T, U_k, S_k). \quad (65)$$

It follows that

$$\begin{aligned} I(W_k, F_{d_k}; Y_k^T | U_k, S_k) &= I(W_k, F_{d_k}; Y_k^T, U_k, S_k) - I(W_k, F_{d_k}; U_k, S_k) \\ &\leq I(W_k, F_{d_k}; Y_j^T, U_k, S_k) - I(W_k, F_{d_k}; U_k, S_k) \end{aligned} \quad (66)$$

$$= I(W_k, F_{d_k}; Y_j^T | U_k, S_k) \quad (67)$$

where the inequality in (66) is due to (65) and the data processing inequality. \square

Equipped with the above lemma and focusing on an arbitrary permutation pair $(p, q) \in \mathcal{P}_s \times \mathcal{P}_N$, the corresponding term on the right-hand-side of (62) is bounded as:

$$\begin{aligned} \sum_{k=1}^s I(W_{p(k)}, F_{q(k)}; Y_{p(k)}^T | U_{p(k)}, S_{p(k)}) &\leq \sum_{k=1}^s I(W_{p(k)}, F_{q(k)}; Y_s^T | U_{p(k)}, S_{p(k)}) \\ &= \sum_{k=1}^s h(Y_s^T | U_{p(k)}, S_{p(k)}) - h(Y_s^T | U_{p(k)}, S_{p(k)}, W_{p(k)}, F_{q(k)}) \\ &\leq \sum_{k=1}^s h(Y_s^T | U_{p(k)}, S_{p(k)}) - h(Y_s^T | U_{p(k+1)}, S_{p(k+1)}) \\ &= h(Y_s^T | U_{p(1)}) - h(Y_s^T | S_{s+1}) \\ &= h(Y_s^T | U_{p(1)}) - h(Z_s^T) \\ &= I(X^T; Y_s^T | U_{p(1)}) \\ &\leq T \log(1 + P^{\alpha_s}). \end{aligned} \quad (68)$$

$$\leq T \log(1 + P^{\alpha_s}). \quad (69)$$

In the above, (68) follows from its preceding equality by recalling that S_{s+1} contains messages and files intended to all users in $[s]$, which map directly to X^T , which is in turn removed from Y_s^T . As (69) holds for all permutations $(p, q) \in \mathcal{P}_s \times \mathcal{P}_N$, and since for any such permutation in (62) we have $\sum_{k \in [s]} R_{p(k)} = \sum_{k \in [s]} R_k$, it follows that each of the inner sums (over k) on the right-hand-side of (62) is bounded by the same term. Therefore, we obtain the bound

$$\begin{aligned} \frac{1}{s!N!} \sum_{(p,q) \in \mathcal{P}_s \times \mathcal{P}_N} \sum_{k=1}^s \left[I(W_{p(k)}, F_{q(k)}; Y_{p(k)}^T | U_{p(k)}, S_{p(k)}) - T(R_{p(k)} - \epsilon_T) \right] &\leq \\ &T \left[\log(1 + P^{\alpha_s}) - \sum_{k=1}^s (R_k - \epsilon_T) \right]. \end{aligned} \quad (70)$$

6.2 Bounding the left-hand-side of (62)

It is evident that for every $k \in [s]$ and $(p, q) \in \mathcal{P}_s \times \mathcal{P}_N$, we have

$$H(F_{q(k)} | U_{p(k)}, S_{p(k)}) = H(F_{q(k)} | U_{p(1)}, \dots, U_{p(k)}, F_{q(1)}, \dots, F_{q(k-1)}), \quad (71)$$

¹¹For rigour, there exists a random variable $\tilde{Y}_j^T \sim Y_j^T$ such that (65) holds while replacing Y_j^T with \tilde{Y}_j^T [42]. Without loss of generality, we use Y_j^T instead of \tilde{Y}_j^T and assume that (65) holds.

which holds since messages are independent of files and cache contents (see (63)). From the equality in (71), it can be seen that the left-hand-side of (62) is in fact a lower bound on the number of bits that must be delivered (i.e load) in a conventional share-link setting with s users, up to a decoding error term [6, eq. (30)]. We hence employ the results and techniques of [6] to obtain:

$$\frac{1}{s!N!} \sum_{(p,q) \in \mathcal{P}_s \times \mathcal{P}_N} \sum_{k=1}^s H(F_{q(k)} | U_{p(k)}, S_{p(k)}) \geq B \cdot \left(s' - 1 + a - \frac{s'(s' - 1) - l(l - 1) + 2as'}{2(N - l + 1)} M \right) \quad (72)$$

$$\geq \frac{B}{2.01} \cdot \left(\frac{N - M}{M} (1 - (1 - M/N)^s) \right) \quad (73)$$

$$\geq \frac{B}{2.01} \cdot \text{conv} \left(\frac{\binom{K}{K\mu+1} - \binom{K-s}{K\mu+1}}{\binom{K}{K\mu}} \right) \quad (74)$$

where the bound in (72) holds for any parameters $s' \in [s]$ and $a \in [0, 1]$, while $l \in [s']$ is the minimum value that satisfies: $(s'(s' - 1) - l(l - 1) + 2as')/2 \leq (N - l + 1)l$. The bound in (72) follows directly from [6, Lem. 3]. On the other hand, going from (72) to within a multiplicative factor of 2.01 from the decentralized load in (73) holds due to [6, Lem. 1]. Finally, the inequality in (74) follows from the results in [5] (see also [6, Appendix G] where a similar step is used).¹²

6.3 Combining bounds

From (62), (70) and (74), and by taking the limit $T \rightarrow \infty$, we obtain

$$\sum_{k=1}^s R_k + \frac{1}{2.01 \cdot \mathcal{T}} \cdot \text{conv} \left(\frac{\binom{K}{K\mu+1} - \binom{K-s}{K\mu+1}}{\binom{K}{K\mu}} \right) \leq \log(1 + P^{\alpha_s}). \quad (75)$$

In the GDoF-GNDT limit, the bound in (75) translates to

$$\sum_{k=1}^s r_k + \frac{1}{2.01 \cdot \tau} \cdot \text{conv} \left(\frac{\binom{K}{K\mu+1} - \binom{K-s}{K\mu+1}}{\binom{K}{K\mu}} \right) \leq \alpha_s. \quad (76)$$

The above holds for any $s \in [\min\{K, N\}]$. These bounds fully describe the lower bound in (26) whenever $N \geq K$. For $N < K$, we require the additional bounds derived next.

6.4 Remaining bounds for $N < K$

Let us now consider a subset of users $[s]$, for some $s \in [\min\{K, N\} + 1 : K]$. Applying the exact above steps to the first N users in $[s]$, which request distinct files, we obtain

$$\frac{B}{2.01} \cdot \text{conv} \left(\frac{\binom{K}{K\mu+1} - \binom{K-N}{K\mu+1}}{\binom{K}{K\mu}} \right) + \sum_{k=1}^N T(R_k - \epsilon_T) \leq \sum_{k=1}^N I(W_{p(k)}, F_{q(k)}; Y_s^T | U_{p(k)}, S_{p(k)}) \quad (77)$$

$$\leq h(Y_s^T | U_{p(1)}) - h(Y_s^T | U_{N+1}, S_{N+1}) \quad (78)$$

The bound in (77) follows from (62) after rearranging, bounding the left-hand-side using (74), and bounding the right-hand-side by fixing a permutation pair (p, q) that maximizes the average. The bound in (78) follows by employing the same steps used to obtain (69).

¹²Note that the lower convex envelope in (74) is defined in a similar manner to (25) in Definition 1.

For the remaining users in $[N + 1 : s]$, let us define their side information variables as

$$S_k = (W_i, F_{d_i}, U_i : i \in [k - 1]). \quad (79)$$

We also use S_{s+1} to denote a side information variable comprising of messages, requested files and cache contents for all users in $[s]$. The non-content sum-rate is bounded above as

$$\sum_{k=N+1}^s T(R_k - \epsilon_T) \leq \sum_{k=N+1}^s I(W_k, F_{d_k}; Y_s^T | U_k, S_k) \quad (80)$$

$$\begin{aligned} &\leq \sum_{k=N+1}^s h(Y_s^T | U_k, S_k) - h(Y_s^T | U_{k+1}, S_{k+1}) \\ &= h(Y_s^T | U_{N+1}, S_{N+1}) - h(Y_s^T | S_{s+1}) \end{aligned} \quad (81)$$

where the inequality in (80) follows from the single user bounds in (59) and Lemma 1. By adding the bounds in (78) and (81), we obtain

$$\frac{B}{2.01} \cdot \text{conv} \left(\frac{\binom{K}{K\mu+1} - \binom{K-N}{K\mu+1}}{\binom{K}{K\mu}} \right) + \sum_{k=1}^s T(R_k - \epsilon_T) \leq h(Y_s^T | U_{p(1)}) - h(Y_s^T | S_{s+1}) \quad (82)$$

$$\leq T \log(1 + P^{\alpha_s}) \quad (83)$$

which in the GDoF-GNDT limit, translates to

$$\sum_{k=1}^s r_k + \frac{1}{2.01 \cdot \tau} \cdot \text{conv} \left(\frac{\binom{K}{K\mu+1} - \binom{K-N}{K\mu+1}}{\binom{K}{K\mu}} \right) \leq \alpha_s. \quad (84)$$

The bound in (84) holds for all $s \in [N + 1 : K]$. By rearranging the terms in (76) and (84), and taking the tightest of such bounds over all $s \in [K]$, we obtain a lower bound given by

$$2.01 \cdot \tau \geq \max_{s \in [K]} \left\{ \frac{1}{(\alpha_s - \sum_{k=1}^s r_k)^+} \cdot \text{conv} \left(\frac{\binom{K}{K\mu+1} - \binom{K - \min\{s, N\}}{K\mu+1}}{\binom{K}{K\mu}} \right) \right\} \quad (85)$$

where there is no loss of generality in incorporating $(\cdot)^+$ in (85) since we have $\sum_{k=1}^s r_k \leq \alpha_s$. The right-hand-side of (85) coincides with $\tau^{\text{ub}}(\mathbf{r}; \mu, \boldsymbol{\alpha})$ in (25). This completes the converse proof.

7 Conclusion

In this work, we introduced the problem of wireless coded caching under mixed cacheable content and uncacheable non-content types of traffic. Focusing on networks in which the physical channel is modelled by a degraded GBC, we proposed a caching and delivery strategy based on the separation principle, which isolates the coded caching and multicasting problem from the physical layer transmission problem. We proved that the proposed strategy achieves near optimal performances in the information-theoretic sense. Through our analysis, we reveal *topological holes* arising due to asymmetries in wireless network topologies, which enable the transmission of non-content messages while incurring no loss in terms of content delivery time. The extension of this result to other networks, including multi-transmitter and multi-antenna networks, is of high interest.

Appendices

A Unicast and Multiple Multicast GDoF Region

In this appendix, we present a proof for Theorem 2.

A.1 Converse

Starting with converse, we invoke Fano's inequality from which we obtain:

$$T(R_i - \epsilon_T) + T \sum_{\mathcal{S} \in \Sigma_i} (R_{\mathcal{S}} - \epsilon_T) \leq I(W_i, \{W_{\mathcal{S}} : \mathcal{S} \in \Sigma_i\}; Y_i^T) \quad (86)$$

$$\leq I(W_i, \{W_{\mathcal{S}} : \mathcal{S} \in \Sigma_i\}; Y_k^T) \quad (87)$$

$$\leq I(W_i, \{W_{\mathcal{S}} : \mathcal{S} \in \Sigma_i\}; Y_k^T | W_i') \quad (88)$$

where T is the number of channel uses over which the communication occurs, ϵ_T is an error term that approaches zero as $T \rightarrow \infty$, and $W_i' \triangleq \{W_j, W_{\mathcal{S}} : \mathcal{S} \in \Sigma_j, j \in [i-1]\}$ is a side information variable. The inequality in (87) holds for all $k \geq i$ due to the degradedness of the physical channel and the order in (10), while (88) holds since W_i' is independent of W_i and $\{W_{\mathcal{S}} : \mathcal{S} \in \Sigma_i\}$.

For any $k \in [K]$, adding up the bounds obtained from (88) for all $i \in [k]$, we obtain

$$\begin{aligned} T \sum_{i \in [k]} (R_i - \epsilon_T) + T \sum_{\mathcal{S} \in \cup_{i \in [k]} \Sigma_i} (R_{\mathcal{S}} - \epsilon_T) &\leq \sum_{i \in [k]} I(W_i, \{W_{\mathcal{S}} : \mathcal{S} \in \Sigma_i\}; Y_k^T | W_i') \\ &= I(\{W_i, W_{\mathcal{S}} : \mathcal{S} \in \Sigma_i, i \in [k]\}; Y_k^T) \\ &\leq T \log(1 + P^{\alpha_k}) \end{aligned} \quad (89)$$

where we implicitly assume that $\Sigma_i = \emptyset$ for all $i \in [K - \sigma + 2 : K]$. From the bound in (89), it follows that the capacity region $\mathcal{C}^{\text{PHY}}(\sigma, \alpha, P)$ is contained in the outer bound $\mathcal{C}_{\text{out}}^{\text{PHY}}(\sigma, \alpha, P)$, described by all rate tuples $(R_k : k \in [K], R_{\mathcal{S}} : \mathcal{S} \in \Sigma) \in \mathbb{R}_+^{K + \binom{K}{\sigma}}$ satisfying:

$$\begin{aligned} \sum_{i \in [k]} R_i + \sum_{\mathcal{S} \in \cup_{i \in [k]} \Sigma_i} R_{\mathcal{S}} &\leq \log(1 + P^{\alpha_k}), \quad \forall k \in [K - \sigma + 1] \\ \sum_{i \in [k]} R_i + \sum_{\mathcal{S} \in \Sigma} R_{\mathcal{S}} &\leq \log(1 + P^{\alpha_k}), \quad \forall k \in [K - \sigma + 2 : K]. \end{aligned} \quad (90)$$

In the GDoF sense, $\mathcal{C}_{\text{out}}^{\text{PHY}}(\sigma, \alpha, P)$ translates to the outer bound denoted by $\mathcal{D}_{\text{out}}^{\text{PHY}}(\sigma, \alpha)$, which coincides with the region characterized by the inequalities in (40).

A.2 Achievability

For the achievability, we use message combining and superposition coding at the transmitter, and successive decoding at the receivers. In particular, we construct K codewords as:

$$\begin{aligned} \{W_k, W_{\mathcal{S}} : \mathcal{S} \in \Sigma_k\} &\rightarrow X_k^T, \quad \forall k \in [K - \sigma + 1] \\ W_k &\rightarrow X_k^T, \quad \forall k \in [K - \sigma + 2 : K] \end{aligned} \quad (91)$$

where each combined message $\{W_k, W_{\mathcal{S}} : \mathcal{S} \in \Sigma_k\}$ has a rate of $R_k + \sum_{\mathcal{S} \in \Sigma_k} R_{\mathcal{S}}$, and each codeword $X_k^T \triangleq (X_k(1), \dots, X_k(T))$ is drawn from an independent Gaussian codebook with unit average

power. The transmit signal $X^T \triangleq (X(1), \dots, X(T))$ is then constructed as:

$$X(t) = \sum_{k \in [K]} \sqrt{q_k} X_k(t) \quad (92)$$

where $q_k \geq 0$ is the power allocated to the k -th codeword, such that $\sum_{k \in [K]} q_k \leq 1$. On the other end, each user k receives the noisy signal: $Y_k(t) = \sqrt{P^{\alpha_k}} \sum_{i \in [K]} \sqrt{q_i} X_i(t) + Z_k(t)$.

Each user $k \in [K]$ decodes the signals $X_1^T, X_2^T, \dots, X_k^T$, successively in that order. Assuming successful decoding, each user k recovers all messages in

$$\{W_i : i \in [k], W_S : \mathcal{S} \in \cup_{i \in [k]} \Sigma_i\} \quad (93)$$

which includes all messages desired by user k , i.e. $\{W_k, W_S : \mathcal{S} \in \Sigma, k \in \mathcal{S}\}$. From the above, it can be seen that each codeword X_k^T is decoded by all users in $[k : K]$, while treating interference from X_{k+1}^T, \dots, X_K^T as noise. Therefore, messages encoded in the signal X_k^T achieve all rates with a sum not exceeding

$$\min_{i \in [k:K]} \left\{ \log \left(1 + \frac{P^{\alpha_i} q_i}{1 + P^{\alpha_i} \sum_{j \in [k+1:K]} q_j} \right) \right\} = \log \left(1 + \frac{P^{\alpha_k} q_k}{1 + P^{\alpha_k} \sum_{j \in [k+1:K]} q_j} \right) \quad (94)$$

where the above equality follows from the fact that $\alpha_k \leq \alpha_i$, for all $i \in [k : K]$. The above described strategy hence achieves the rate region described by all non-negative rate tuples that satisfy

$$\begin{aligned} R_k + \sum_{\mathcal{S} \in \Sigma_k} R_{\mathcal{S}} &\leq \log \left(1 + \frac{P^{\alpha_k} q_k}{1 + P^{\alpha_k} \sum_{j \in [k+1:K]} q_j} \right), \quad \forall k \in [K - \sigma + 1] \\ R_k &\leq \log \left(1 + \frac{P^{\alpha_k} q_k}{1 + P^{\alpha_k} \sum_{j \in [k+1:K]} q_j} \right), \quad \forall k \in [K - \sigma + 2 : K] \end{aligned} \quad (95)$$

for some feasible power allocation $\mathbf{q} \triangleq (q_1, \dots, q_K)$.

We now obtain an inner bound on the above achievable rate region which is more malleable for GDoF and constant-gap analysis. To this end, we adopt the following power allocation:

$$\begin{aligned} q_k &= P^{-\beta_k} - P^{-\beta_{k+1}}, \quad \forall k \in [K - 1] \\ q_K &= P^{-\beta_K} \end{aligned} \quad (96)$$

where the sequence of power exponents in (96) satisfies:

$$0 = \beta_1 \leq \beta_2 \leq \dots \leq \beta_K \quad \text{and} \quad \beta_{k+1} \leq \alpha_k, \quad \forall k \in [K - 1]. \quad (97)$$

Recalling that $P > 1$, it can be verified that the above power allocation is feasible, and satisfies:

$$\sum_{j \in [k:K]} q_j = P^{-\beta_k}, \quad \forall k \in [K]. \quad (98)$$

Using this power allocation, the rate in (94) is bounded below for all $k \in [K - 1]$ as:

$$\log \left(1 + \frac{P^{\alpha_k} q_k}{1 + P^{\alpha_k} \sum_{j \in [k+1:K]} q_j} \right) = \log \left(\frac{1 + P^{\alpha_k} \sum_{i \in [k:K]} q_j}{1 + P^{\alpha_k} \sum_{j \in [k+1:K]} q_j} \right) \quad (99)$$

$$= \log \left(\frac{1 + P^{\alpha_k} P^{-\beta_k}}{1 + P^{\alpha_k} P^{-\beta_{k+1}}} \right) \quad (100)$$

$$\geq \log \left(\max \left\{ 1, \frac{P^{\beta_{k+1} - \beta_k}}{2} \right\} \right) \quad (101)$$

$$= ((\beta_{k+1} - \beta_k) \log(P) - 1)^+. \quad (102)$$

For $k = K$, we obtain the same bound by setting $\beta_{K+1} = \alpha_K$, i.e.

$$\log(1 + P^{\alpha_K} q_K) = \log \left(1 + P^{\beta_{K+1} - \beta_K} \right) \geq ((\beta_{K+1} - \beta_K) \log(P) - 1)^+. \quad (103)$$

This yields the inner bound $\mathcal{C}_{\text{in}}^{\text{PHY}}(\sigma, \boldsymbol{\alpha}, P)$, described by all non-negative rate tuples that satisfy:

$$R_k + \sum_{\mathcal{S} \in \Sigma_k} R_{\mathcal{S}} \leq ((\beta_{k+1} - \beta_k) \log(P) - 1)^+, \quad \forall k \in [K - \sigma + 1] \quad (104)$$

$$R_k \leq ((\beta_{k+1} - \beta_k) \log(P) - 1)^+, \quad \forall k \in [K - \sigma + 2 : K]$$

for some feasible power exponents $\boldsymbol{\beta} \triangleq (\beta_1, \dots, \beta_K)$, as defined in (97). In the GDoF sense, $\mathcal{C}_{\text{in}}^{\text{PHY}}(\sigma, \boldsymbol{\alpha}, P)$ translates to $\mathcal{D}_{\text{in}}^{\text{PHY}}(\sigma, \boldsymbol{\alpha})$, described by all non-negative GDoF tuples that satisfy:

$$r_k + \sum_{\mathcal{S} \in \Sigma_k} r_{\mathcal{S}} \leq \beta_{k+1} - \beta_k, \quad \forall k \in [K - \sigma + 1] \quad (105)$$

$$r_k \leq \beta_{k+1} - \beta_k, \quad \forall k \in [K - \sigma + 2 : K]$$

for some feasible power allocation $\boldsymbol{\beta}$. By definition, we have $\mathcal{D}_{\text{in}}^{\text{PHY}}(\sigma, \boldsymbol{\alpha}) \subseteq \mathcal{D}_{\text{out}}^{\text{PHY}}(\sigma, \boldsymbol{\alpha})$. Nevertheless, it turns out that the two regions coincide as shown through the following result.

Lemma 2. *The achievable GDoF region $\mathcal{D}_{\text{in}}^{\text{PHY}}(\sigma, \boldsymbol{\alpha})$ and the outer bound $\mathcal{D}_{\text{out}}^{\text{PHY}}(\sigma, \boldsymbol{\alpha})$ are equal.*

Lemma 2 is proved by eliminating all power allocation variables in (105) using means of Fourier-Motzkin elimination. This yields an equivalent representation of $\mathcal{D}_{\text{in}}^{\text{PHY}}(\sigma, \boldsymbol{\alpha})$ that coincides with the inequalities in (40), and hence $\mathcal{D}_{\text{out}}^{\text{PHY}}(\sigma, \boldsymbol{\alpha})$. It follows that

$$\mathcal{D}_{\text{in}}^{\text{PHY}}(\sigma, \boldsymbol{\alpha}) = \mathcal{D}_{\text{out}}^{\text{PHY}}(\sigma, \boldsymbol{\alpha}) = \mathcal{D}^{\text{PHY}}(\sigma, \boldsymbol{\alpha}) \quad (106)$$

which completes the proof of Theorem 2. Next, we present the proof of Lemma 2.

A.3 Proof of Lemma 2

For convenience, let us define the new GDoF variables $\boldsymbol{\rho} \triangleq (\rho_1, \dots, \rho_K)$ as

$$\rho_k \triangleq r_k + \sum_{\mathcal{S} \in \Sigma_k} r_{\mathcal{S}}, \quad \forall k \in [1 : K - \sigma + 1] \quad (107)$$

$$\rho_k \triangleq r_k, \quad \forall k \in [K - \sigma + 2 : K].$$

The achievable GDoF region $\mathcal{D}_{\text{in}}^{\text{PHY}}(\sigma, \boldsymbol{\alpha})$ is described by the following sets of inequalities:

$$\rho_k \leq \beta_{k+1} - \beta_k, \quad \forall k \in [K] \quad (108)$$

$$0 \leq \alpha_k - \beta_{k+1}, \quad \forall k \in [K - 1] \quad (109)$$

$$0 \leq \beta_{k+1} - \beta_k, \quad \forall k \in [K - 1] \quad (110)$$

which capture both GDoF conditions in (105), as well as conditions on power allocation variables in (97). Note that since $\rho_k \geq 0$, the set of inequalities in (110) is redundant and hence can be ignored. We now proceed to eliminate β_2, \dots, β_K (recall that $\beta_1 = 0$ and $\beta_{K+1} = \alpha_K$) using a Fourier-Motzkin procedure, see, e.g., [42, Appendix D]. This is carried out sequentially, eliminating $\beta_K, \beta_{K-1}, \dots, \beta_2$ in that order. Starting with β_K , relevant inequalities are given by

$$0 \leq \alpha_{K-1} - \beta_K \quad (111)$$

$$\rho_K \leq \alpha_K - \beta_K \quad (112)$$

$$\rho_{K-1} \leq \beta_K - \beta_{K-1}. \quad (113)$$

We eliminate β_K by adding each of the inequalities with $-\beta_K$ on the right-hand-side, i.e. (111) and (112), to the inequality with β_K on the right-hand-side, i.e. (113). This yields

$$\begin{aligned} \rho_{K-1} &\leq \alpha_{K-1} - \beta_{K-1} \\ \rho_K + \rho_{K-1} &\leq \alpha_K - \beta_{K-1}. \end{aligned} \quad (114)$$

After the elimination of β_K , we are left with the following inequalities

$$\begin{aligned} \rho_k &\leq \beta_{k+1} - \beta_k, \quad \forall k \in [K-2] \\ \rho_{K-1} &\leq \alpha_{K-1} - \beta_{K-1} \\ \rho_K + \rho_{K-1} &\leq \alpha_K - \beta_{K-1} \\ 0 &\leq \alpha_k - \beta_{k+1}, \quad \forall k \in [K-2]. \end{aligned} \quad (115)$$

Next, we eliminate β_{K-1} . To this end, we isolate the following inequalities

$$\begin{aligned} 0 &\leq \alpha_{K-2} - \beta_{K-1} \\ \rho_{K-1} &\leq \alpha_{K-1} - \beta_{K-1} \\ \rho_K + \rho_{K-1} &\leq \alpha_K - \beta_{K-1} \\ \rho_{K-2} &\leq \beta_{K-1} - \beta_{K-2} \end{aligned} \quad (116)$$

from which we eliminate β_{K-1} and obtain

$$\begin{aligned} \rho_{K-2} &\leq \alpha_{K-2} - \beta_{K-2} \\ \rho_{K-1} + \rho_{K-2} &\leq \alpha_{K-1} - \beta_{K-2} \\ \rho_K + \rho_{K-1} + \rho_{K-2} &\leq \alpha_K - \beta_{K-2}. \end{aligned} \quad (117)$$

After eliminating β_{K-1} , we are left with the following set of inequalities

$$\begin{aligned} \rho_k &\leq \beta_{k+1} - \beta_k, \quad \forall k \in [K-3] \\ \rho_{K-2} &\leq \alpha_{K-2} - \beta_{K-2} \\ \rho_{K-1} + \rho_{K-2} &\leq \alpha_{K-1} - \beta_{K-2} \\ \rho_K + \rho_{K-1} + \rho_{K-2} &\leq \alpha_K - \beta_{K-2} \\ 0 &\leq \alpha_k - \beta_{k+1}, \quad \forall k \in [K-3]. \end{aligned} \quad (118)$$

Proceeding in a similar manner, it can be verified that after the E -th elimination, where $E \in [K-2]$, we are left with the following set of inequalities:

$$\begin{aligned} \rho_k &\leq \beta_{k+1} - \beta_k, \quad \forall k \in [K-E-1] \\ \rho_{K-E} &\leq \alpha_{K-E} - \beta_{K-E} \\ &\vdots \\ \rho_K + \rho_{K-1} + \dots + \rho_{K-E} &\leq \alpha_K - \beta_{K-E} \\ 0 &\leq \alpha_k - \beta_{k+1}, \quad \forall k \in [K-E-1] \end{aligned} \quad (119)$$

which after the $(K - 2)$ -th elimination, boils down to

$$\begin{aligned}
\rho_1 &\leq \beta_2 \\
\rho_2 &\leq \alpha_2 - \beta_2 \\
\rho_3 + \rho_2 &\leq \alpha_3 - \beta_2 \\
&\vdots \\
\rho_K + \rho_{K-1} + \cdots + \rho_2 &\leq \alpha_K - \beta_2 \\
0 &\leq \alpha_1 - \beta_2.
\end{aligned} \tag{120}$$

Finally, we eliminate β_2 in (120), from which we obtain

$$\begin{aligned}
\rho_1 &\leq \alpha_1 \\
\rho_2 + \rho_1 &\leq \alpha_2 \\
&\vdots \\
\rho_K + \rho_{K-1} + \cdots + \rho_2 + \rho_1 &\leq \alpha_K.
\end{aligned} \tag{121}$$

It is evident that the set of inequalities in (121) is identical to the set of inequalities that describe $\mathcal{D}^{\text{PHY}}(\sigma, \boldsymbol{\alpha})$ in (40), which completes the proof of Lemma 2.

A.4 Constant gap

Here we show that the GDoF region characterization in Lemma 2 translates to an approximate characterization of the capacity region. The tools used to establish this result are reused further on in Appendix D to establish a similar result for the original cache-aided channel.

Corollary 4. The capacity region $\mathcal{C}^{\text{PHY}}(\sigma, \boldsymbol{\alpha}, P)$ includes all non-negative rate tuples that satisfy

$$\begin{aligned}
\sum_{i \in [k]} R_i + \sum_{\mathcal{S} \in \cup_{i \in [k]} \Sigma_i} R_{\mathcal{S}} &\leq (\alpha_k \log(P) - k)^+, \quad \forall k \in [K - \sigma + 1] \\
\sum_{i \in [k]} R_i + \sum_{\mathcal{S} \in \Sigma} R_{\mathcal{S}} &\leq (\alpha_k \log(P) - k)^+, \quad \forall k \in [K - \sigma + 2 : K].
\end{aligned} \tag{122}$$

Moreover, this achievable region is within 2 bits (per dimension) from the entire capacity region for all system parameters. That is, for any tuple $(R_k : k \in [K], R_{\mathcal{S}} : \mathcal{S} \in \Sigma)$ at the boundary of (122), the tuple $(R_k + 2 : k \in [K], R_{\mathcal{S}} + 2 : \mathcal{S} \in \Sigma)$ is outside the capacity region $\mathcal{C}^{\text{PHY}}(\sigma, \boldsymbol{\alpha}, P)$.

Proof. First, we observe from (105) and Lemma 2 that the achievable rate region $\mathcal{C}_{\text{in}}^{\text{PHY}}(\sigma, \boldsymbol{\alpha}, P)$, described in (104), is equivalently expressed by the set of all non-negative rate tuples that satisfy

$$\begin{aligned}
R_k + \sum_{\mathcal{S} \in \Sigma_k} R_{\mathcal{S}} &\leq \left(r_k \log(P) + \sum_{\mathcal{S} \in \Sigma_k} r_{\mathcal{S}} \log(P) - 1 \right)^+, \quad \forall k \in [K - \sigma + 1] \\
R_k &\leq (r_k \log(P) - 1)^+, \quad \forall k \in [K - \sigma + 2 : K]
\end{aligned} \tag{123}$$

for some $(r_k : k \in [K], r_{\mathcal{S}} : \mathcal{S} \in \Sigma) \in \mathcal{D}^{\text{PHY}}(\sigma, \boldsymbol{\alpha})$. Next, we show that (123) includes the achievable rate region describe in (122). Suppose that $(R_k : k \in [K], R_{\mathcal{S}} : \mathcal{S} \in \Sigma)$ satisfies (122) in Corollary 4. From Lemma 2, there must exist ρ_1, \dots, ρ_K , as defined in (107), such that

$$\sum_{i \in [k]} R_i + \sum_{\mathcal{S} \in \cup_{i \in [k]} \Sigma_i} R_{\mathcal{S}} = \left(\sum_{i \in [k]} \rho_i \log(P) - k \right)^+ \leq (\alpha_k \log(P) - k)^+, \quad \forall k \in [K] \tag{124}$$

where in the above, we have used $\Sigma_i = \emptyset$ for all $i \in [K - \sigma + 2 : K]$. This implies that

$$\begin{aligned} R_k + \sum_{\mathcal{S} \in \cup_k \Sigma_k} R_{\mathcal{S}} &= \left[\sum_{i \in [k]} R_i + \sum_{\mathcal{S} \in \cup_{i \in [k]} \Sigma_i} R_{\mathcal{S}} \right] - \left[\sum_{i \in [k-1]} R_i + \sum_{\mathcal{S} \in \cup_{i \in [k-1]} \Sigma_i} R_{\mathcal{S}} \right] \\ &\leq \left(\sum_{i \in [k]} \rho_i \log(P) - k \right)^+ - \left(\sum_{i \in [k-1]} \rho_i \log(P) - (k-1) \right) \\ &\leq (\rho_k \log(P) - 1)^+. \end{aligned} \quad (125)$$

Therefore, $(R_k : k \in [K], R_{\mathcal{S}} : \mathcal{S} \in \Sigma)$ satisfies (123), and hence is in $\mathcal{C}_{\text{in}}^{\text{PHY}}(\sigma, \alpha, P)$.

Now let us consider a rate tuple $(R'_k : k \in [K], R'_{\mathcal{S}} : \mathcal{S} \in \Sigma)$ at the boundary of the rate region in (122). It follows that there exists some k' in $[K]$ such that (122) holds with equality, that is

$$\sum_{i \in [k']} R'_i + \sum_{\mathcal{S} \in \cup_{i \in [k']} \Sigma_i} R'_{\mathcal{S}} = (\alpha_{k'} \log(P) - k')^+. \quad (126)$$

Now consider a second rate tuple given by

$$(R''_k = R'_k + 2 : k \in [K], R''_{\mathcal{S}} = R'_{\mathcal{S}} + 2 : \mathcal{S} \in \Sigma). \quad (127)$$

For the index k' in (126), we have

$$\begin{aligned} \sum_{i \in [k']} R''_i + \sum_{\mathcal{S} \in \cup_{i \in [k']} \Sigma_i} R''_{\mathcal{S}} &= \sum_{i \in [k']} R'_i + \sum_{\mathcal{S} \in \cup_{i \in [k']} \Sigma_i} R'_{\mathcal{S}} + 2 \cdot \left(k' + \sum_{i \in [k']} |\Sigma_i| \right) \\ &\geq \alpha_{k'} \log(P) - k' + 2 \cdot \left(k' + \sum_{i \in [k']} |\Sigma_i| \right) \\ &\geq \alpha_{k'} \log(P) + 1. \end{aligned} \quad (128)$$

The inequality in (128) implies that the rate tuple defined in (127) is not included in the outer bound $\mathcal{C}_{\text{out}}^{\text{PHY}}(\sigma, \alpha, P)$. This holds since the inequalities in (90) imply:

$$\sum_{i \in [k]} R_i + \sum_{\mathcal{S} \in \cup_{i \in [k]} \Sigma_i} R_{\mathcal{S}} < \log(P^{\alpha_k}) + 1, \quad \forall k \in [K] \quad (129)$$

where strictness in the above inequalities is due to $P > 1$ and $\alpha_k > 0$, for all $k \in [K]$. Moreover, as alluded to in Remark 2, for the regime $P \leq 1$, the all zero rate tuple is within one bit (per dimension) from all rate tuples in $\mathcal{C}_{\text{out}}^{\text{PHY}}(\sigma, \alpha, P)$. This concludes the proof of Corollary 4. \square

B Non-Integer $K\mu$

In this appendix, we prove that the GNDT in (25) is achievable for all μ such that $K\mu$ is non-integer. Therefore, we assume throughout this appendix that $K\mu$ takes a non-integer value in $(0, K)$. Moreover, we focus on worst-case demands as defined in Section 5.2.

B.1 Physical channel

We first look at the physical channel problem. In particular, let us consider a degraded GBC with three message sets: a unicast set, a σ -multicast set and a γ -multicast, where $\sigma, \gamma \in [2 : K]$ and

$\sigma < \gamma$. Similar to the definitions of Σ and Σ_i for the σ -multicast groups in Section 4.1, we denote the set of all γ -multicast groups by Γ , which is partitioned into $\{\Gamma_i : i \in [K - \gamma + 1]\}$. The GDoF region of this channel is hence given by all GDoF tuples of the form

$$(r_k : k \in [K], r_S : S \in \Sigma, r_G : G \in \Gamma) \in \mathbb{R}_+^{K + \binom{K}{\sigma} + \binom{K}{\gamma}}$$

which satisfy the following set of inequalities:

$$\sum_{i \in [k]} r_i + \sum_{S \in \cup_{i \in [k]} \Sigma_i} r_S + \sum_{G \in \cup_{j \in [k]} \Gamma_j} r_G \leq \alpha_k, \forall k \in [K] \quad (130)$$

where we assume that $\Sigma_i = \emptyset$ for all $i \in [K - \sigma + 2 : K]$, and $\Gamma_j = \emptyset$ for all $j \in [K - \gamma + 2 : K]$. The proof of (130) follows the same steps used to prove Theorem 2 in Appendix A, and is omitted to avoid repetition. Similar to Corollary 3, the GDoF region in (130) yields the lower dimensional projection characterized by all tuples $(r_k : k \in [K], r_{\text{sym}}^\sigma, r_{\text{sym}}^\gamma) \in \mathbb{R}_+^{K+2}$ that satisfy

$$\sum_{i \in [k]} r_i + \left[\binom{K}{\sigma} - \binom{K - \min\{k, s\}}{\sigma} \right] \cdot r_{\text{sym}}^\sigma + \left[\binom{K}{\gamma} - \binom{K - \min\{k, s\}}{\gamma} \right] \cdot r_{\text{sym}}^\gamma \leq \alpha_k, \forall k \in [K] \quad (131)$$

which captures scenarios with symmetric σ -multicast GDoF and symmetric γ -multicast GDoF, where each multicast message is intended to at least one users in $[s]$, for some $s \in [K]$.

B.2 Caching and Delivery

We introduce some notation which is used in the following parts. Recalling that $K\mu$ is non-integer, we set the multicast group sizes as: $\sigma = \lfloor K\mu + 1 \rfloor$ and $\gamma = \lceil K\mu + 1 \rceil$. Moreover, we define the following fractions: $\lambda \triangleq \gamma - (K\mu + 1)$ and $\bar{\lambda} \triangleq (K\mu + 1) - \sigma$, where it is evident that $\bar{\lambda} = 1 - \lambda$.

Content placement, preparing the coded multicast messages and recovering files at the receivers is carried out in the YMA manner, using the principle of memory-sharing [3, 5, 6]. The problem reduces to delivering a set of σ -multicast messages, γ -multicast messages and unicast messages. It is worthwhile noting that due to file splitting during the placement phase and memory-sharing, each of the σ -multicast messages has a normalized file size of $\lambda / \binom{K}{\sigma-1}$, while each γ -multicast message has a normalized file size of $\bar{\lambda} / \binom{K}{\gamma-1}$. From (131), it follows that for any achievable GDoF tuple $(\mathbf{r}, r_{\text{sym}}^\sigma, r_{\text{sym}}^\gamma)$, where \mathbf{r} comprises the GDoF of non-content messages, a GNDT given by

$$\tau = \max \left\{ \frac{\lambda}{r_{\text{sym}}^\sigma \cdot \binom{K}{\sigma-1}}, \frac{\bar{\lambda}}{r_{\text{sym}}^\gamma \cdot \binom{K}{\gamma-1}} \right\} \quad (132)$$

is achievable. The point-wise maximum in (132) is due to the fact that the GNDT is determined by the *slowest* group of coded content messages. We further optimize the symmetric σ -multicast GDoF and the symmetric γ -multicast GDoF such that they satisfy

$$r_{\text{sym}}^\sigma = r_{\text{sym}}^\gamma \cdot \frac{\lambda \binom{K}{\gamma-1}}{\bar{\lambda} \binom{K}{\sigma-1}}. \quad (133)$$

In this case, (132) boils down to

$$\tau = \frac{\lambda}{r_{\text{sym}}^\sigma \cdot \binom{K}{\sigma-1}} = \frac{\bar{\lambda}}{r_{\text{sym}}^\gamma \cdot \binom{K}{\gamma-1}} \quad (134)$$

and for any achievable τ , we achieve the GDoF region given by all $\mathbf{r} \in \mathbb{R}_+^K$ that satisfy

$$\frac{1}{\tau} \cdot \left(\lambda \cdot \frac{\binom{K}{\sigma} - \binom{K - \min\{k, N\}}{\sigma}}{\binom{K}{\sigma-1}} + \bar{\lambda} \cdot \frac{\binom{K}{\gamma} - \binom{K - \min\{k, N\}}{\gamma}}{\binom{K}{\gamma-1}} \right) + \sum_{i \in [k]} r_i \leq \alpha_k, \quad \forall k \in [K]. \quad (135)$$

This translates to an achievable GNDT of

$$\tau = \max_{k \in [K]} \left\{ \frac{1}{(\alpha_k - \sum_{i \in [k]} r_i)^+} \cdot \left(\lambda \cdot \frac{\binom{K}{\sigma} - \binom{K - \min\{k, N\}}{\sigma}}{\binom{K}{\sigma-1}} + \bar{\lambda} \cdot \frac{\binom{K}{\gamma} - \binom{K - \min\{k, N\}}{\gamma}}{\binom{K}{\gamma-1}} \right) \right\}. \quad (136)$$

Now it remains to show that (136) and (25) are equal for all non-integer values of $K\mu$.

To this end, let us recall from [6, Appendix J] that for any $k \in [K]$, the sequence defined as

$$c_n \triangleq \frac{\binom{K}{n+1} - \binom{K - \min\{k, N\}}{n+1}}{\binom{K}{n}} \quad (137)$$

is convex in $n \in [0 : K]$. Therefore, the points defined by (137) are corner points on their lower convex envelope given by $f(n) = \text{conv}(c_n)$, and cannot be expressed as convex combinations of other points on $f(n)$ (see also [5, Remark 7]). Hence for any non-integer value of n in $(0, K)$, we have $f(n) = (\lceil n \rceil - n)f(\lfloor n \rfloor) + (n - \lfloor n \rfloor)f(\lceil n \rceil)$. This is precisely the expression appearing inside the $\max\{\cdot\}$ operator in (136), from which it directly follows that (136) and (25) are equal.

B.3 Proof of (35)

In the final part of this appendix, we show that the inequality in (35) holds. First, that due to the convexity of the sequence in (137), the new sequence given by

$$C_n \triangleq \max_{k \in [K]} \left\{ \frac{1}{(\alpha_k - \sum_{i \in [k]} r_i)^+} \cdot \frac{\binom{K}{n+1} - \binom{K - \min\{k, N\}}{n+1}}{\binom{K}{n}} \right\} \quad (138)$$

is also convex in $n \in [0 : K]$. This holds since the point-wise maximum of convex functions is a convex function. Therefore, the conclusions made about lower convex envelope $f(n) = \text{conv}(c_n)$ above also hold for the lower convex envelope $F(n) = \text{conv}(C_n)$.

From the above, it follows that $\tau_{\text{ms}}^{\text{ub}}(\mathbf{r}; \mu, \boldsymbol{\alpha}) = \tau^{\text{ub}}(\mathbf{r}; \mu, \boldsymbol{\alpha})$ for all μ such that $K\mu$ takes integer values. Moreover, for non-integer value of $K\mu$, the function $\tau_{\text{ms}}^{\text{ub}}(\mathbf{r}; \mu, \boldsymbol{\alpha})$ can be expressed as

$$\begin{aligned} \tau_{\text{ms}}^{\text{ub}}(\mathbf{r}; \mu, \boldsymbol{\alpha}) &= \lambda \cdot \max_{k \in [K]} \left\{ \frac{1}{(\alpha_k - \sum_{i \in [k]} r_i)^+} \cdot \frac{\binom{K}{\sigma} - \binom{K - \min\{k, N\}}{\sigma}}{\binom{K}{\sigma-1}} \right\} \\ &\quad + \bar{\lambda} \cdot \max_{k \in [K]} \left\{ \frac{1}{(\alpha_k - \sum_{i \in [k]} r_i)^+} \cdot \frac{\binom{K}{\gamma} - \binom{K - \min\{k, N\}}{\gamma}}{\binom{K}{\gamma-1}} \right\} \\ &\geq \max_{k \in [K]} \left\{ \frac{1}{(\alpha_k - \sum_{i \in [k]} r_i)^+} \cdot \left(\lambda \cdot \frac{\binom{K}{\sigma} - \binom{K - \min\{k, N\}}{\sigma}}{\binom{K}{\sigma-1}} + \bar{\lambda} \cdot \frac{\binom{K}{\gamma} - \binom{K - \min\{k, N\}}{\gamma}}{\binom{K}{\gamma-1}} \right) \right\}. \quad (139) \end{aligned}$$

The inequity in (139), which is identical to the inequality in (35), is implied by Jensen's inequality, as the point-wise maximum function $\max\{\cdot\}$ is convex in its arguments.

C Non-Worst-Case Demands

Here we show that the trade-off in (57), shown to be achievable in Section 5 when the weakest users make distinct demands, is also achieved whenever the distinct demands are not made by the weakest users. In particular, we consider the case where $N < K$ with N distinct demands, yet these distinct demands are not necessarily made by the first N users. Whenever $N \geq K - \sigma + 1$, we transmit the set of all coded multicast messages and achieve the delay in (57). Therefore, we focus on the case where $N \leq K - \sigma$, in which not all coded multicast messages are transmitted. Recall that placement is independent of user demands, and hence remains as in Section 5.

C.1 Coded multicast messages:

After user demands are revealed, we select the set of leading users as $\mathcal{U} = \{u_1, \dots, u_N\}$, such that $u_1 \leq u_2 \leq \dots \leq u_N$, and each u_i is the weakest users (i.e. smallest index) that requests file $F_{d_{u_i}}$. Note that we must have $u_1 = 1$. The set of non-leading users is given by $\bar{\mathcal{U}} = [K] \setminus \mathcal{U}$. Generating coded multicast messages is carried out as in the previous part, in accordance with the YMA scheme, where each generated message is useful to at least one leading user. The generated set of coded multicast messages is given by $\{W_{\mathcal{S}} : \mathcal{S} \in \Sigma, \mathcal{S} \cap \mathcal{U} \neq \emptyset\}$.

Let us, for now, assume that leading users successfully decode their intended coded multicast messages, and hence recover their requested files. We show that in this case, non-leading users will also be able to compute their missing coded multicast messages, and recover their requested files.

Lemma 3. *Given that each transmitted coded multicast message $W_{\mathcal{S}}$ is successfully decoded by all intended users in \mathcal{S} , then each non-leading user $k \in \bar{\mathcal{U}}$ can compute all required missing coded multicast messages, i.e. $\{W_{\mathcal{A}} : \mathcal{A} \subseteq \bar{\mathcal{U}}, |\mathcal{A}| = \sigma, k \in \mathcal{A}\}$.*

Proof. Consider an arbitrary missing coded multicast message $W_{\mathcal{A}}$, for some group of non-leading users $\mathcal{A} = \{a_1, \dots, a_{\sigma}\} \subseteq \bar{\mathcal{U}}$, which we wish to compute. We assume without loss of generality that $a_1 = \min\{\mathcal{A}\}$, i.e. the weakest user in the group \mathcal{A} . To show that users in \mathcal{A} can compute $W_{\mathcal{A}}$, it is sufficient to show that a_1 can compute $W_{\mathcal{A}}$. Next, we show that each of the transmitted coded multicast messages required for computing $W_{\mathcal{A}}$ is either intended to leading users which are no stronger than user a_1 or intended to user a_1 ; and hence decodable by all users in \mathcal{A} .

To this end, let u_j be the leading user that satisfies $u_j < a_1 < u_{j+1}$. If $j = N$, then a_1 is stronger than all leading users and hence can recover all their intended messages. Combining this with the fact that $u_1 = 1$, we may proceed while assuming that there exists a pair of users u_j and u_{j+1} in \mathcal{U} such that $u_j < a_1 < u_{j+1}$ holds. The file demanded by user a_1 , i.e. $F_{d_{a_1}}$, must also be demanded by some user $u' \in \{u_1, \dots, u_j\}$, since otherwise a_1 must be a leading user. In reconstructing $W_{\mathcal{A}}$ according to (55), we define $\mathcal{B} = \{u_1, \dots, u_N, a_1, \dots, a_{\sigma}\}$, and Υ as the family of subsets of \mathcal{B} that constitute potential sets of leaders, other than \mathcal{U} .

The problem reduced to showing that each $\mathcal{B} \setminus \mathcal{V}$, where $\mathcal{V} \in \Upsilon$, contains at least one user from $\{u_1, \dots, u_j, a_1\}$. To show this, first consider the case where $a_1 \in \mathcal{V}$. Here we must have $u' \notin \mathcal{V}$ and therefore $u' \in \mathcal{B} \setminus \mathcal{V}$, which proves the statement in Lemma 3. Now let us consider the second case where $a_1 \notin \mathcal{V}$. If $u' \notin \mathcal{V}$ also holds, i.e. there is a third user demanding $F_{d_{a_1}}$ and is in \mathcal{V} , then Lemma 3 holds, and therefore we focus on the remaining case where $u' \in \mathcal{V}$. In this case, a_1 cannot be in \mathcal{V} , and hence we must have $a_1 \in \mathcal{B} \setminus \mathcal{V}$, which completes the proof. \square

It is worthwhile highlighting that an observation similar to Lemma 3 was made in [10, Rem. 2]. Following Lemma 3, we now focus on the transmission of the sets of messages $\{W_k : k \in [K]\}$ and $\{W_{\mathcal{S}} : \mathcal{S} \in \Sigma, \mathcal{S} \cap \mathcal{U} \neq \emptyset\}$, and characterize the corresponding achievable performance.

C.2 Transmission

The sets of coded multicast messages and unicast messages are transmitted using the physical-layer scheme in Section 4. Next, we show that (57) is also achievable in this case by deriving an upper bound on the achievable GNDT, given any achievable GDoF tuple \mathbf{r} , which matches the one in (57). To this end, we define a new family of subsets of Σ as

$$\Sigma'_{u_i} \triangleq \{\mathcal{S} \in \Sigma : u_i \in \mathcal{S}, u_j \notin \mathcal{S}, \forall j \in [i-1]\} \quad (140)$$

It follows that the set of coded multicast messages of interest can be described by

$$\{W_{\mathcal{S}} : \mathcal{S} \in \Sigma, \mathcal{S} \cap \mathcal{U} \neq \emptyset\} = \{W_{\mathcal{S}} : \mathcal{S} \in \cup_{i \in [N]} \Sigma'_{u_i}\}. \quad (141)$$

We now focus on transmission over the physical channel in Section 4. By setting the achievable GDoF for all missing σ -multicast messages to zero, and restricting to a symmetric GDoF across remaining σ -multicast messages, the GDoF region in Theorem 2 becomes

$$\begin{aligned} \sum_{i \in [k]} r_i &\leq \alpha_k, \quad \forall k \in [u_1 - 1] \\ \sum_{i \in [k]} r_i + \left| \bigcup_{i \in [j]} \Sigma'_{u_i} \right| \cdot r_{\text{sym}} &\leq \alpha_k, \quad \forall k \in [u_j : u_{j+1} - 1], j \in [N - 1] \\ \sum_{i \in [k]} r_i + \left| \bigcup_{i \in [N]} \Sigma'_{u_i} \right| \cdot r_{\text{sym}} &\leq \alpha_k, \quad \forall k \in [u_N : K]. \end{aligned} \quad (142)$$

Next, we observe that for each leading user $u_i \in \mathcal{U}$, we must have $i \leq u_i$. It follows that the symmetric σ -multicast GDoF region in (142) includes the achievable region given by

$$\begin{aligned} \sum_{i \in [k]} r_i + \left| \bigcup_{i \in [k]} \Sigma'_{u_i} \right| \cdot r_{\text{sym}} &\leq \alpha_k, \quad \forall k \in [N - 1] \\ \sum_{i \in [k]} r_i + \left| \bigcup_{i \in [N]} \Sigma'_{u_i} \right| \cdot r_{\text{sym}} &\leq \alpha_k, \quad \forall k \in [N : K]. \end{aligned} \quad (143)$$

The above holds as for each $k \in [K]$, the corresponding inequality in (143) implies its counterpart inequality in (142). Employing a calculation similar to the one in (49), it can be shown that $|\cup_{i \in [k]} \Sigma'_{u_i}| = \binom{K}{\sigma} - \binom{K-k}{\sigma}$, for all $k \in [N]$. Therefore, it follows from (143) that for any unicast GDoF tuple $(r_k : k \in [K])$, an achievable symmetric multicast GDoF is given by

$$r_{\text{sym}} \leq \min_{k \in [K]} \left\{ \frac{(\alpha_k - \sum_{i \in [k]} r_i)^+}{\binom{K}{\sigma} - \binom{K - \min\{k, N\}}{\sigma}} \right\} \quad (144)$$

from which we conclude that the GNDT-GDoF trade-off in (57) is achievable in this case as well.

D Approximate Delay-Rate Characterization

In this appendix, we show that the optimal GNDT-GDoF characterization in Corollary 2 (and Theorem 1) leads to an approximate optimal delay-rate characterization, as stated in Remark 8.

Corollary 5. The capacity region $\mathcal{C}(\mathcal{T}; \mu, \boldsymbol{\alpha}, P)$ includes all non-negative rate tuples that satisfy

$$\sum_{i \in [k]} R_i + \frac{1}{\mathcal{T}} \cdot \text{conv} \left(\frac{\binom{K}{K\mu+1} - \binom{K-\min\{k, N\}}{K\mu+1}}{\binom{K}{K\mu}} \right) \leq (\alpha_k \log(P) - k)^+, \forall k \in [K]. \quad (145)$$

Moreover, for any delay-rate tuple $(\mathcal{T}, \mathbf{R}'; \mu)$ such that $\mathbf{R}' = (R'_1, \dots, R'_K)$ is at the boundary of the achievable region described in (145), the best any scheme can do is to increase each rate R'_k by less than 2 bits per channel use, and reduce \mathcal{T}' by at most a multiplicative factor of 2.01.

Proof. Following the same steps in Appendix A.4, and combining with the achievability arguments in Section 5 and Appendix B, it can be verified that $\mathcal{C}(\mathcal{T}; \mu, \boldsymbol{\alpha}, P)$ includes the achievable rate region described above in (145). On the other hand, the same argument used to show (129) in Appendix A.4 can be employed to show that the outer bound derived in Section 6 implies that any rate tuple in $\mathcal{C}(\mathcal{T}; \mu, \boldsymbol{\alpha}, P)$ must satisfy

$$\sum_{i \in [k]} R_i + \frac{1}{2.01 \cdot \mathcal{T}} \cdot \text{conv} \left(\frac{\binom{K}{K\mu+1} - \binom{K-\min\{k, N\}}{K\mu+1}}{\binom{K}{K\mu}} \right) < \alpha_k \log(P) + 1, \forall k \in [K]. \quad (146)$$

Now let us introduce the rate tuple $\mathbf{R}'' = (R''_1, \dots, R''_K) = (R'_1 + 2, \dots, R'_K + 2)$ and the delay $\mathcal{T}'' = \mathcal{T}/2.01$. Since \mathbf{R}' is at the boundary of the region in (145), we must have an index $k' \in [K]$ such that at least one of the inequalities in (145) holds with equality. This implies that

$$\begin{aligned} \sum_{i \in [k']} R''_i + \frac{1}{2.01 \cdot \mathcal{T}''} \cdot \text{conv} \left(\frac{\binom{K}{K\mu+1} - \binom{K-\min\{k', N\}}{K\mu+1}}{\binom{K}{K\mu}} \right) \\ = \sum_{i \in [k']} R'_i + \frac{1}{\mathcal{T}'} \cdot \text{conv} \left(\frac{\binom{K}{K\mu+1} - \binom{K-\min\{k', N\}}{K\mu+1}}{\binom{K}{K\mu}} \right) + 2k' \\ = (\alpha_{k'} \log(P) - k')^+ + 2k' \end{aligned} \quad (147)$$

$$\geq \alpha_{k'} \log(P) + 1. \quad (148)$$

It follows from (146) and (148) that \mathbf{R}'' is strictly outside the capacity region $\mathcal{C}(\mathcal{T}''; \mu, \boldsymbol{\alpha}, P)$, and therefore the delay-rate tuple $(\mathcal{T}'', \mathbf{R}''; \mu)$ is in fact not achievable. \square

References

- [1] G. S. Paschos, G. Iosifidis, M. Tao, D. Towsley, and G. Caire, “The role of caching in future communication systems and networks,” *IEEE J. Sel. Areas Commun.*, vol. 36, no. 6, pp. 1111–1125, Jun. 2018.
- [2] K. Shanmugam, N. Golrezaei, A. G. Dimakis, A. F. Molisch, and G. Caire, “Femtocaching: Wireless content delivery through distributed caching helpers,” *IEEE Trans. Inf. Theory*, vol. 59, no. 12, pp. 8402–8413, Dec. 2013.
- [3] M. A. Maddah-Ali and U. Niesen, “Fundamental limits of caching,” *IEEE Trans. Inf. Theory*, vol. 60, no. 5, pp. 2856–2867, May 2014.
- [4] K. Wan, D. Tuninetti, and P. Piantanida, “On the optimality of uncoded cache placement,” in *Proc. IEEE ITW*, Sep. 2016, pp. 161–165.

- [5] Q. Yu, M. A. Maddah-Ali, and A. S. Avestimehr, “The exact rate-memory tradeoff for caching with uncoded prefetching,” *IEEE Trans. Inf. Theory*, vol. 64, no. 2, pp. 1281–1296, Feb. 2018.
- [6] —, “Characterizing the rate-memory tradeoff in cache networks within a factor of 2,” *IEEE Trans. Inf. Theory*, vol. 65, no. 1, pp. 647–663, Jan. 2019.
- [7] S. P. Shariatpanahi, S. A. Motahari, and B. H. Khalaj, “Multi-server coded caching,” *IEEE Trans. Inf. Theory*, vol. 62, no. 12, pp. 7253–7271, Dec. 2016.
- [8] A. Ghorbel, M. Kobayashi, and S. Yang, “Content delivery in erasure broadcast channels with cache and feedback,” *IEEE Trans. Inf. Theory*, vol. 62, no. 11, pp. 6407–6422, Nov. 2016.
- [9] M. M. Amiri and D. Gündüz, “Cache-aided content delivery over erasure broadcast channels,” *IEEE Trans. Commun.*, vol. 66, no. 1, pp. 370–381, Jan. 2018.
- [10] —, “Caching and coded delivery over Gaussian broadcast channels for energy efficiency,” *IEEE J. Sel. Areas Commun.*, vol. 36, no. 8, pp. 1706–1720, Aug. 2018.
- [11] —, “On the capacity region of a cache-aided Gaussian broadcast channel with multi-layer messages,” in *Proc. IEEE ISIT*, Jun. 2018, pp. 1909–1913.
- [12] M. Salman and M. K. Varanasi, “The exact capacity-memory tradeoff for caching with uncoded prefetching in the two-receiver Gaussian broadcast channel,” in *Proc. IEEE ISIT*, Jul. 2019, pp. 1222–1226.
- [13] S. S. Bidokhti, M. Wigger, and A. Yener, “Benefits of cache assignment on degraded broadcast channels,” *arXiv:1702.08044*, 2017.
- [14] S. S. Bidokhti, M. Wigger, and R. Timo, “Noisy broadcast networks with receiver caching,” *IEEE Trans. Inf. Theory*, vol. 64, no. 11, pp. 6996–7016, Nov. 2018.
- [15] J. Zhang and P. Elia, “Wireless coded caching: A topological perspective,” in *Proc. IEEE ISIT*, Jun. 2017, pp. 401–405.
- [16] E. Lampiris, J. Zhang, O. Simeone, and P. Elia, “Fundamental limits of wireless caching under uneven-capacity channels,” *arXiv:1908.04036*, 2019.
- [17] J. Zhang, F. Engelmann, and P. Elia, “Coded caching for reducing CSIT-feedback in wireless communications,” in *Proc. Allerton*, Sep. 2015, pp. 1099–1105.
- [18] J. Zhang and P. Elia, “Fundamental limits of cache-aided wireless BC: Interplay of coded-caching and CSIT feedback,” *IEEE Trans. Inf. Theory*, vol. 63, no. 5, pp. 3142–3160, May 2017.
- [19] E. Piovano, H. Joudeh, and B. Clerckx, “On coded caching in the overloaded MISO broadcast channel,” in *Proc. IEEE ISIT*, Jun. 2017, pp. 2795–2799.
- [20] K. Ngo, S. Yang, and M. Kobayashi, “Scalable content delivery with coded caching in multi-antenna fading channels,” *IEEE Trans. Wireless Commun.*, vol. 17, no. 1, pp. 548–562, Jan 2018.
- [21] E. Lampiris and P. Elia, “Achieving full multiplexing and unbounded caching gains with bounded feedback resources,” in *Proc. IEEE ISIT*, Jun. 2018, pp. 1440–1444.

- [22] E. Piovano, H. Joudeh, and B. Clerckx, “Generalized degrees of freedom of the symmetric cache-aided MISO broadcast channel with partial CSIT,” *IEEE Trans. Inf. Theory*, vol. 65, no. 9, pp. 5799–5815, Sep. 2019.
- [23] I. Bergel and S. Mohajer, “Cache-aided communications with multiple antennas at finite SNR,” *IEEE J. Sel. Areas Commun.*, vol. 36, no. 8, pp. 1682–1691, Aug. 2018.
- [24] S. P. Shariatpanahi, G. Caire, and B. Hossein Khalaj, “Physical-layer schemes for wireless coded caching,” *IEEE Trans. Inf. Theory*, vol. 65, no. 5, pp. 2792–2807, May 2019.
- [25] Y. Cao and M. Tao, “Treating content delivery in multi-antenna coded caching as general message sets transmission: A DoF region perspective,” *IEEE Trans. Wireless Commun.*, vol. 18, no. 6, pp. 3129–3141, Jun. 2019.
- [26] M. Ji, G. Caire, and A. F. Molisch, “Fundamental limits of caching in wireless D2D networks,” *IEEE Trans. Inf. Theory*, vol. 62, no. 2, pp. 849–869, Feb. 2016.
- [27] M. A. Maddah-Ali and U. Niesen, “Cache-aided interference channels,” in *Proc. IEEE ISIT*, Jun. 2015, pp. 809–813.
- [28] N. Naderializadeh, M. A. Maddah-Ali, and A. S. Avestimehr, “Fundamental limits of cache-aided interference management,” *IEEE Trans. Inf. Theory*, vol. 63, no. 5, pp. 3092–3107, May 2017.
- [29] F. Xu, M. Tao, and K. Liu, “Fundamental tradeoff between storage and latency in cache-aided wireless interference networks,” *IEEE Trans. Inf. Theory*, vol. 63, no. 11, pp. 7464–7491, Nov. 2017.
- [30] Y. Cao, M. Tao, F. Xu, and K. Liu, “Fundamental storage-latency tradeoff in cache-aided MIMO interference networks,” *IEEE Trans. Wireless Commun.*, vol. 16, no. 8, pp. 5061–5076, Aug. 2017.
- [31] J. Hachem, U. Niesen, and S. N. Diggavi, “Degrees of freedom of cache-aided wireless interference networks,” *IEEE Trans. Inf. Theory*, vol. 64, no. 7, pp. 5359–5380, Jul. 2018.
- [32] E. Lampiris, J. Zhang, and P. Elia, “Cache-aided cooperation with no CSIT,” in *Proc. IEEE ISIT*, Jun. 2017, pp. 2960–2964.
- [33] E. Piovano, H. Joudeh, and B. Clerckx, “Centralized and decentralized cache-aided interference management in heterogeneous parallel channels,” *IEEE Trans. Commun.*, to appear.
- [34] A. Sengupta, R. Tandon, and O. Simeone, “Fog-aided wireless networks for content delivery: Fundamental latency tradeoffs,” *IEEE Trans. Inf. Theory*, vol. 63, no. 10, pp. 6650–6678, Oct. 2017.
- [35] J. Zhang and O. Simeone, “Fundamental limits of cloud and cache-aided interference management with multi-antenna edge nodes,” *IEEE Trans. Inf. Theory*, vol. 65, no. 8, pp. 5197–5214, Aug. 2019.
- [36] E. Lampiris and P. Elia, “Adding transmitters dramatically boosts coded-caching gains for finite file sizes,” *IEEE J. Sel. Areas Commun.*, vol. 36, no. 6, pp. 1176–1188, Jun. 2018.
- [37] E. Parrinello, A. Ünsal, and P. Elia, “Fundamental limits of coded caching with multiple antennas, shared caches and uncoded prefetching,” *IEEE Trans. Inf. Theory*, to appear.

- [38] G. Paschos, E. Bastug, I. Land, G. Caire, and M. Debbah, “Wireless caching: technical misconceptions and business barriers,” *IEEE Commun. Magazine*, vol. 54, no. 8, pp. 16–22, Aug. 2016.
- [39] R. H. Etkin, D. N. C. Tse, and H. Wang, “Gaussian interference channel capacity to within one bit,” *IEEE Trans. Inf. Theory*, vol. 54, no. 12, pp. 5534–5562, Dec. 2008.
- [40] G. Bresler, A. Parekh, and D. N. C. Tse, “The approximate capacity of the many-to-one and one-to-many Gaussian interference channels,” *IEEE Trans. Inf. Theory*, vol. 56, no. 9, pp. 4566–4592, Sep. 2010.
- [41] S. A. Jafar and S. Vishwanath, “Generalized degrees of freedom of the symmetric Gaussian K user interference channel,” *IEEE Trans. Inf. Theory*, vol. 56, no. 7, pp. 3297–3303, Jul. 2010.
- [42] A. El Gamal and Y.-H. Kim, *Network information theory*. Cambridge university press, 2011.